doi : 10.17596/0002978

KAIYO Cruise Report

KY13-16

Thermal structure of the Philippine Sea plate subducting along the Nankai Trough and its relation to seismic activity

Nankai Trough and Shikoku Basin

October 27, 2013 – November 6, 2013

Japan Agency for Marine-Earth Science and Technology
(JAMSTEC)

Contents

1. Cruise Information

Cruise number:
KY13-16

Ship name:
R/V KAIYO

Title of the cruise:
Thermal structure of the Philippine Sea plate subducting along the Nankai Trough and its relation to seismic activity

Title of proposal:
Thermal structure of the Philippine Sea plate subducting along the Nankai Trough and its relation to seismic activity

Cruise period:
October 27, 2013 – November 6, 2013

Port call:
2013 Oct. 27 Dept. from Yokosuka
Dec. 6 Arriv. at Wakayama

Research area:
Nankai Trough and Shikoku Basin

Research map:

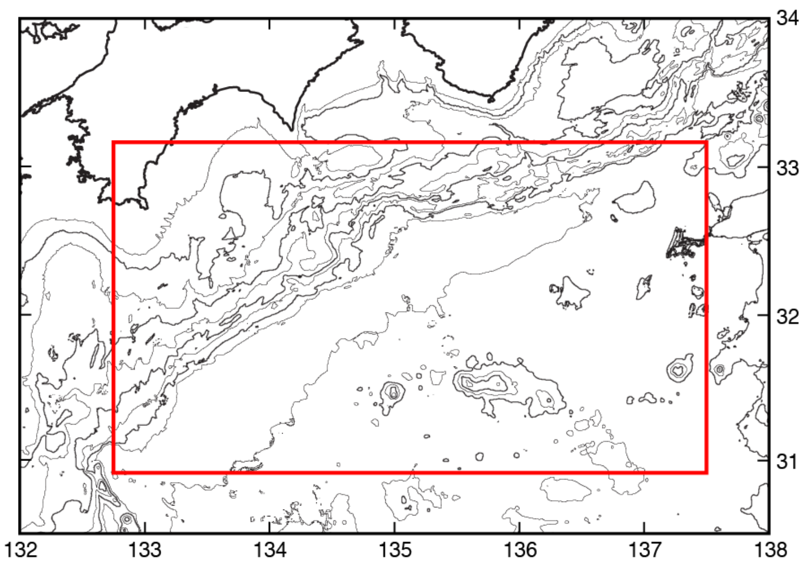

Figure 1-1. Proposed research area of KY13-16 cruise.

Ship track and observation points are shown in 3.2.3.

2. Researchers

Chief Scientist:

Makoto YAMANO	Earthquake Research Institute, University of Tokyo	

Science Party:

Makoto YAMANO	Earthquake Research Institute, University of Tokyo	
Minoru IKEHARA	Center for Advanced Marine Core Research, Kochi University	
Shusaku GOTO	Institute for Geo-Resources and Environment National Institute of Advanced Industrial Science and Technology	
Chikaaki FUJITA	Earthquake Research Institute, University of Tokyo	
Yoshifumi KAWADA	Earthquake Research Institute, University of Tokyo	
Mika SATA	Faculty of Science, Kochi University	
Tsuyoshi KOGA	Faculty of Science, Yamaguchi University	
Arata NAKAJIMA	Faculty of Science, Yamaguchi University	
Kazushige OBARA	Earthquake Research Institute, University of Tokyo	(shore-based)
Kimihiro MOCHIZUKI	Earthquake Research Institute, University of Tokyo	(shore-based)
Kiichiro KAWAMURA	Graduate School of Science and Engineering Yamaguchi University	(shore-based)
Takeshi TSUJI	International Institute for Carbon-Neutral Energy Research Kyushu University	(shore-based)
Masataka KINOSHITA	Kochi Institute for Core Sample Research Japan Agency for Marine-Earth Science and Technology	(shore-based)
Toshiya KANAMATSU	Institute for Research on Earth Evolution Japan Agency for Marine-Earth Science and Technology	(shore-based)
Akiko TANAKA	Institute of Geology and Geoinformation National Institute of Advanced Industrial Science and Technology	(shore-based)
Hideki HAMAMOTO	Center for Environmental Science in Saitama	(shore-based)

Technical Support Staff

Masayuki TOIZUMI	Nippon Marine Enterprises, Ltd.
Hiroyuki HAYASHI	Marine Works Japan, Ltd.
Yuki MIYAJIMA	Marine Works Japan, Ltd.
Yasumi YAMADA	Marine Works Japan, Ltd.
Mika YAMAGUCHI	Marine Works Japan, Ltd.

3. Observation

3.1. Introduction

The temperature structure of the subducting oceanic plate, generally determined by the seafloor age, is one of the most important factors controlling the subsurface thermal structure of subduction zones. In the Nankai subduction zone, the age of the subducting Philippine Sea plate (Shikoku Basin) significantly varies along the trough in a range of about 15 to 30 m.y. (e.g., Okino et al., 1994). The thermal structure of the plate interface and the overriding plate should accordingly vary along the trough. Surface heat flow observed on the floor of the Nankai Trough is, however, not consistent with the age of the Shikoku Basin, indicating that the temperature structure of the Shikoku Basin lithosphere may be different from that expected from the seafloor age. Off eastern Shikoku (off Muroto), the mean of heat flow on the trough floor is extremely high, about 200 mW/m^2, twice as high as the value corresponding to the age (15 m.y.) taking account of the effect of sedimentation (Yamano et al., 2003). In contrast, the values observed in the area southeast of the Kii Peninsula (off Kumano) are around 100 mW/m^2, close to the value estimated from the age (20 m.y.) with the sedimentation effect (Hamamoto et al., 2011). It is important to investigate what is the cause of this difference for studies of the thermal structure of the Nankai subduction zone.

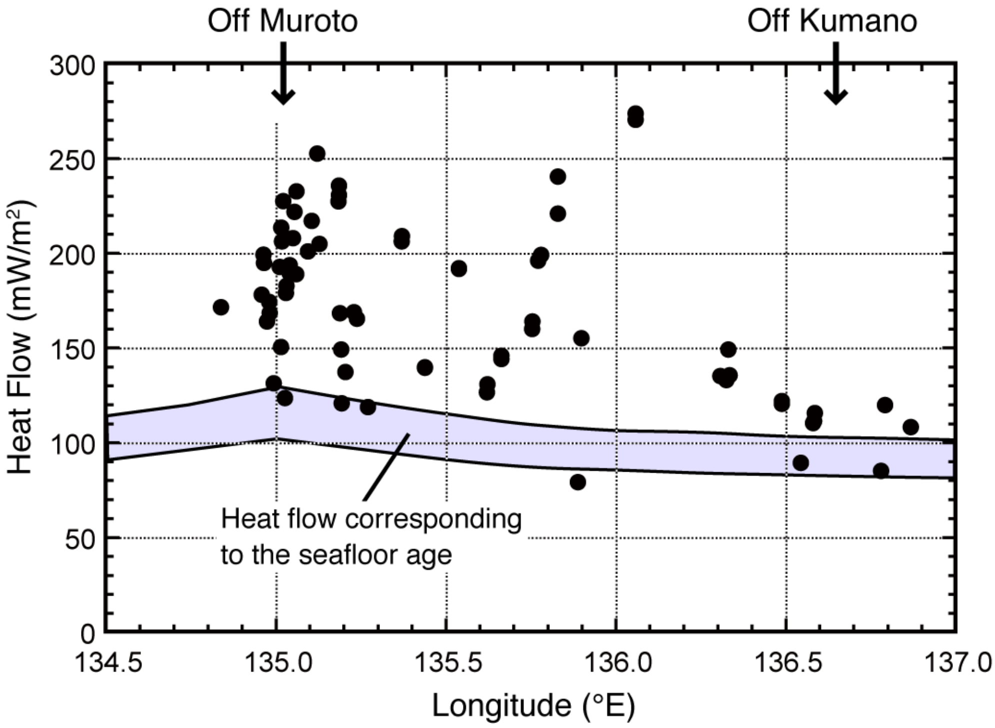

Figure 3.1-1. Heat flow data on the floor of the Nankai Trough plotted versus the longitude. Compared to the value estimated from the age of the subducting Shikoku Basin, heat flow is anomalously high off Muroto, while it is normal off Kumano.

We conducted heat flow measurements on the floor of the Nankai Trough between the off-Muroto and off-Kumano areas (south of the Kii Peninsula) in order to examine the transition from high to normal heat flow for investigation of the cause of the high anomaly and the thermal structure of the Shikoku Basin lithosphere. The obtained data show that extremely high heat flow is observed in the area west of 136°E, where heat flow is highly variable and the mean value is comparable to that in the off-Muroto area (Fig. 3.1-1). The boundary between the western high heat flow area and the eastern normal heat flow area was not clear because the data was still rather sparse.

In 2011, we made concentrated heat flow measurements on the trough floor south of the Kii Peninsula. The results suggest that the heat flow distribution boundary is rather sharp and located in the close vicinity of 136°E. The 136°E boundary is close to the rupture segmentation boundary between the 1944 Tonankai and the 1946 Nankai earthquakes, across which seismicity on the landward side of the trough conspicuously changes (Mochizuki et al., 2010). It also coincides with the transform boundary between the youngest part of the Shikoku Basin formed by spreading in NE-SW direction and the older part formed by E-W spreading, indicating that some physical difference between the younger and older Shikoku Basin may have yielded a contrast in the thermal structure. This possible relationship can be examined through heat flow measurements on the trough floor to the west of the off-Muroto area, where another boundary between the younger and older Shikoku Basin is located.

A likely cause of the anomalous high heat flow in the area off Muroto and west of 136°E is advective heat transfer by hydrothermal circulation in the Shikoku Basin oceanic crust. The uppermost several hundred meters of the basaltic basement of the oceanic crust generally has high permeability and allows extensive pore fluid flow (e.g., Fisher, 2005). Hydrothermal circulation may therefore be occurring in a high permeability layer just below impermeable sediments in the Shikoku Basin crust as well, influencing the temperature structure of the upper part of the plate and surface heat flow (Yamano et al., 1992). For example, sharp landward decrease in heat flow in the frontal part of the accretionary prism off Muroto (Fig. 3.1-2) cannot be caused by a conductive process and must be associated with some advective heat transfer.

Spinelli and Wang (2008) proposed the following model to explain the high heat flow anomaly off Muroto. The topmost part of the Shikoku Basin oceanic crust retains high permeability even after subduction and allows vigorous pore fluid flow which efficiently transfers heat along the plate interface from deeper part of the subduction zone. The upward advective heat transfer results in high heat flow on the Nankai Trough floor (Fig. 3.1-2) and cools down the plate interface (seismogenic zone of great subduction thrust earthquakes). If we apply this model to the heat flow distribution on the trough floor, the transition from the high heat flow off Muroto to the normal heat flow off Kumano may correspond to variation in the upward heat transfer by pore fluid flow, which may results from a difference in the permeability structure between the younger and older Shikoku Basin oceanic crust.

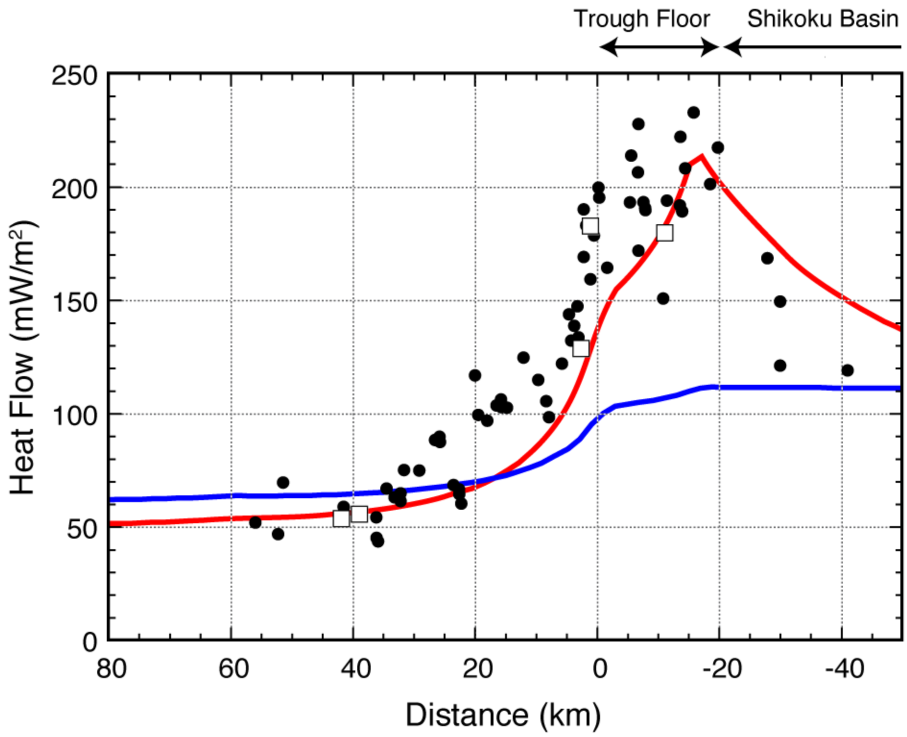

Figure 3.1-2. Heat flow profile across the Nankai Trough off Muroto (Yamano et al., 2003). The horizontal axis is the distance from the deformation front (positive landward). Red and blue curves are surface heat flow calculated with the model of Spinelli and Wang (2008) with vigorous fluid circulation in the subducting crust and with no circulation respectively.

3.2. Summary of the Cruise

3.2.1. Research items

(1) Heat flow measurement (HF)

Measurement of temperature profiles in surface sediment with ordinary deep-sea heat flow probes for determination of terrestrial heat flow.

(2) Sediment core sampling (HFPC, GC)

Sampling of surface sediments with a piston corer and heat flow measurement at the same site using small temperature recorders mounted on the core barrel, or simple sediment sampling with a gravity corer.

(3) Bathymetry survey

Bathymetry mapping with a multi narrow beam system.

3.2.2. Cruise schedule and operations

Date	Events, Operations
Oct. 27	Leave Yokosuka Transit to the survey area
Oct. 28	Arrive in the survey area Heat flow measurement (HF01)
Oct. 29	Piston core sampling with heat flow measurement (HFPC01) Heat flow measurement (HF02) Bathymetry survey
Oct. 30	Heat flow measurement (HF03) Heat flow measurement (HF04) Bathymetry survey
Oct. 31	Gravity core sampling (GC01) Heat flow measurement (HF05) Bathymetry survey
Nov. 1	Heat flow measurement (HF06) Heat flow measurement (HF07) Bathymetry survey
Nov. 2	Piston core sampling with heat flow measurement (HFPC02) Heat flow measurement (HF08) Bathymetry survey
Nov. 3	Piston core sampling with heat flow measurement (HFPC03) Heat flow measurement (HF09) Bathymetry survey
Nov. 4	Heat flow measurement (HF10) Heat flow measurement (HF11) Bathymetry survey
Nov. 5	Heat flow measurement (HF12) Heat flow measurement (HF13) Leave the survey area
Nov. 6	Arrive at Wakayama

Detailed cruise log is given in 7.1.

3.2.3. Ship track and observation points

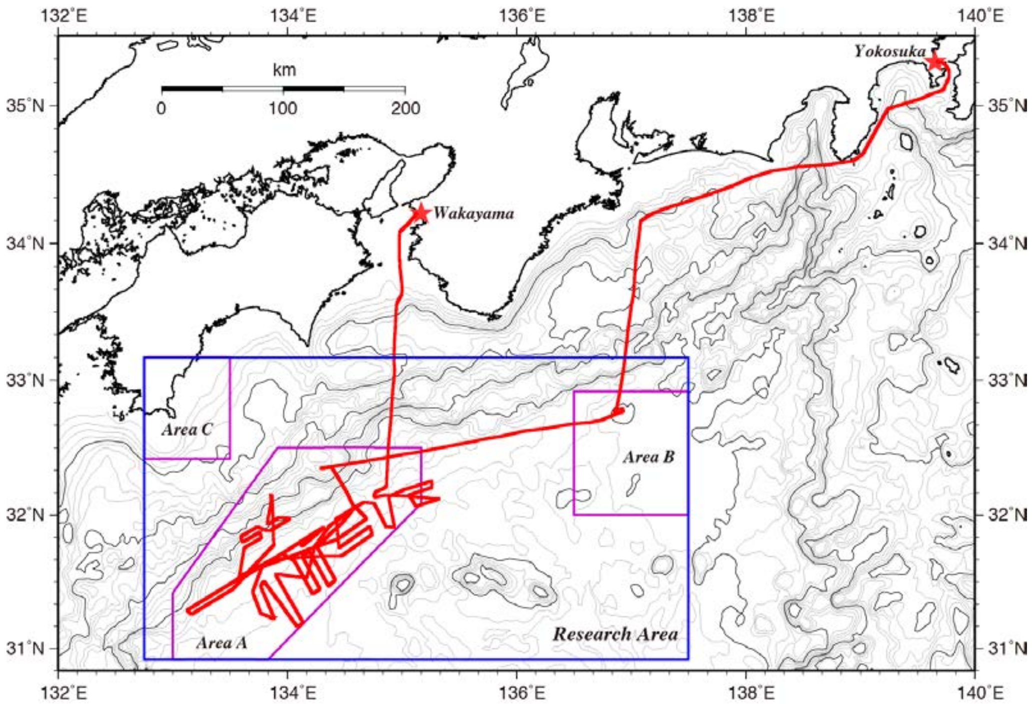

Figure 3.2-1. Research area and ship track of KY13-16 cruise.

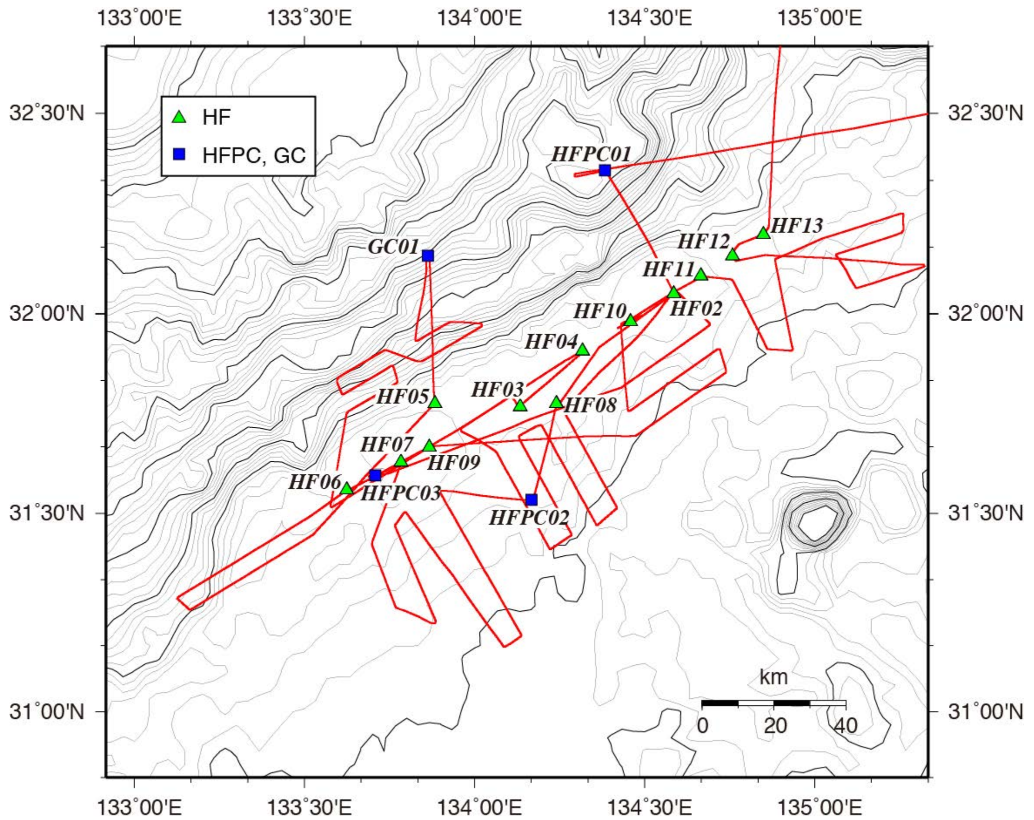

Figure 3.2-2. Measurement and sampling stations in the area A.

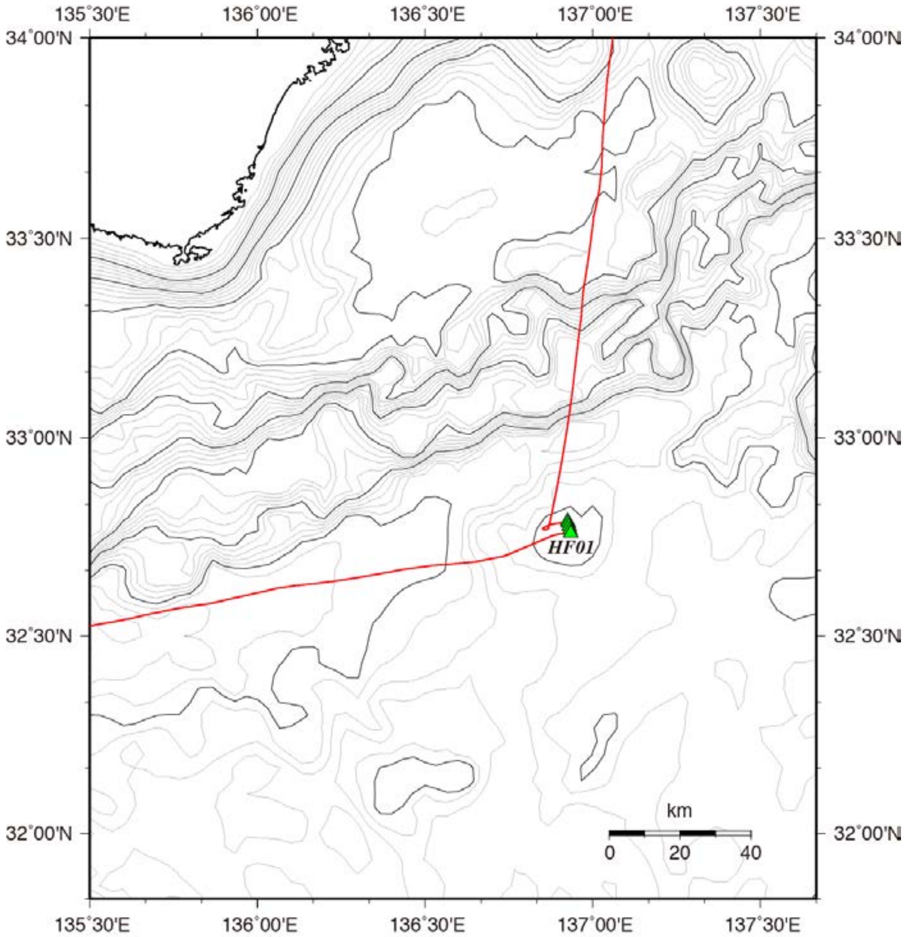

Figure 3.2-3. Measurement stations in the area B.

3.3. Research Objectives

We conduct heat flow measurements in the Nankai Trough off Shikoku and the Kii Peninsula and in the northernmost part of the Shikoku Basin. Detailed measurements on the floor of the Nankai Trough allow us to reveal variation of heat flow along the trough axis. We can then discuss a possible relationship between the heat flow distribution on the trough floor and the structure of the subducting Shikoku Basin crust. In the Shikoku Basin, we examine the influence of a basement high (Kashinosaki Knoll) on the heat flow distribution. Comparing the obtained data with results of numerical modeling, we evaluate heat transfer by pore fluid flow in the upper part of the oceanic crust and investigate how seismic activity and deformation process in the Nankai subduction zone is related to the temperature structure around the subductio plate interface, which may be controlled by the structure of the subducting plate. Sediment core samples taken for thermal property measurements are used for studies on the past variation of the Kuroshio current as well.

Specific objectives of this research cruise

(1) Heat flow measurement on the Nankai Trough floor

We investigate heat flow distribution on the floor of Nankai Trough south of Shikoku, west of 135°E (Area A in Fig. 3.2-1). Recent heat flow surveys on the trough floor south of the Kii Peninsula, including measurements made on the NT11-23 cruise, showed that the average and variability of heat flow significantly change around 136°E, which may correspond to a structure boundary in the subducting Shikoku Basin oceanic crust (Yamano et al., 2012). Measurements in the area south of Shikoku will reveal the overall heat flow distribution on the Nankai Trough floor between 133° and 137°E. It can be compared with along-arc variations in other geophysical features of the subduction zone, e.g., seismicity (e.g., Obana et al., 2006), slow earthquakes (Obara, 2011), age and crustal structure of the subducting Shikoku Basin (Okino et al., 1994; Ike et al, 2008), and magnetic anomaly (Kido and Fujiwara, 2004).

(2) Heat flow measurement in the Shikoku Basin

We conduct heat flow measurements on and around the Kashinosaki Knoll, a prominent bathymetric high located in the northernmost part of the Shikoku Basin off the Kii Peninsula (Area B in Fig. 3.2-1). Temperature measurements in IDOP drill holes showed heat flow near the crest of the knoll (C0012) is significantly higher than the value at the foot (C0011), indicating heat transfer by fluid flow in the basement of the knoll (Henry et al., 2012). Additional surface heat flow measurements on and the around the knoll provide information on the fluid flow scheme.

(3) Measurement of thermal properties of sediment core samples

We take sediment core samples using a piston corer and measure thermal properties of core samples (Area A in Fig. 3.2-1). Measurement of thermal conductivity is particularly important for determination of heat flow. Information on sedimentation rate and depositional environment deduced from samples is also useful for interpretation of the obtained heat flow values.

(4) Geochemical and micropaleontological studies of sediment core samples

The Kuroshio is a western boundary current of the North Pacific subtropical gyre and plays a role of main heat transport from the tropical ocean to the subarctic Pacific. Therefore, it seems that the changes of path and intensity of the Kuroshio in the Northwest Pacific influenced the climate changes in the East Asia, biological production (Ikehara et al., 2009), upper ocean thermal structure (Sagawa et al., 2011) and distribution of marine sediments in this region. We take sediment cores using a piston corer and a gravity corer in the Nankai Trough and the surrounding area (Area A in Fig. 3.2-1). The taken sediment cores will be provided for geochemical and micropaleontological studies in order to understand past variations of the Kuroshio flow axis, meandering history of the Kuroshio, marine productivity, and carbonate dissolution. In addition, we plan to investigate the distribution and thickness of the widespread tephra (Kikai-Akahoya: K-Ah, Aira-Tn: AT, and others) (Ikehara et al., 2006) in the Northwest Pacific.

3.4. Instruments and Operation Methods

3.4.1. Deep-sea heat flow probe

Heat flow is obtained as the product of the geothermal gradient and the thermal conductivity. We measured the geothermal gradient by penetrating an ordinary deep-sea heat flow probe or a heat flow piston corer (HFPC, cf. 3.4.2) into seafloor sediments.

[Specification of tools]

The deep-sea heat flow probe (Fig. 3.4-1) weighs about 800 kg and has a 3.0 m-long lance, along which seven compact temperature recorders (Miniaturized Temperature Data Logger, ANTARES Datensysteme GmbH; Fig. 3.4-2) are mounted in an outrigger fashion (Ewing type). A heat flow data logger (Kaiyo Denshi Co., DHF-650) placed inside the weight head (cf. Fig. 3.4-3) was used for recording the tilt and the depth of the probe.

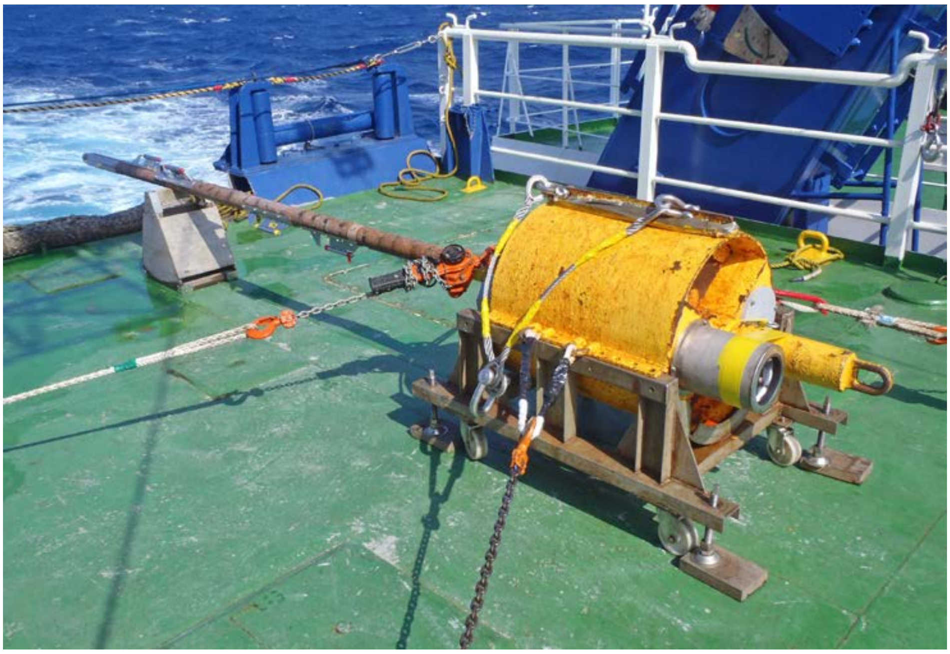

Figure 3.4-1. Deep-sea heat flow probe.

Figure 3.4-2. ANTARES Miniaturized Temperature Data Logger (MTL).

Specifications of the heat flow data logger and the ANTARES Miniaturized Temperature Data Logger (MTL) are summarized below:

Heat Flow Data Logger DHF-650 (Kaiyo Denshi Co.)

Pressure case: titanium alloy

Case length: 725 mm

Maximum diameter: 145 mm

Pressure rating: 7000 m water depth

Tilt: two-axis, 0 to ±45°

Data-cycle interval: 30 sec

Miniaturized Temperature Data Logger (ANTARES Datensysteme GmbH)

Pressure case: stainless steel

Case length: 160 mm

Diameter: 15 mm

Pressure rating: 6000 m water depth

Number of temperature channel: 1

Temperature resolution: 1.2 mK at 20°C, 0.75 mK at 1°C

Sample rate: variable from 1 sec to 255 min.

[Operations]

A 15 m long nylon rope was inserted between the heat flow probe and the winch wire rope in order not to kink the wire rope during probe penetrations. An acoustic transponder was attached about 70 m above the probe for precise determination of the position of the probe (Fig. 3.4-3).

Multi-penetration heat-flow measurement operations were conducted following the procedures described below.

1. Measure water temperature about 50 m above the seafloor for calibration of the temperature recorders.
2. Lower the probe at a speed of about 1 m/sec until it penetrates into the sediment.
3. Measure temperatures in the sediment for about 15 min. Monitor the wire tension and pay out the wire when necessary to keep the probe stable.
4. Pull out the probe.
5. Move to the next station keeping the probe about 300 m above the seafloor.
6. Repeat penetrations.

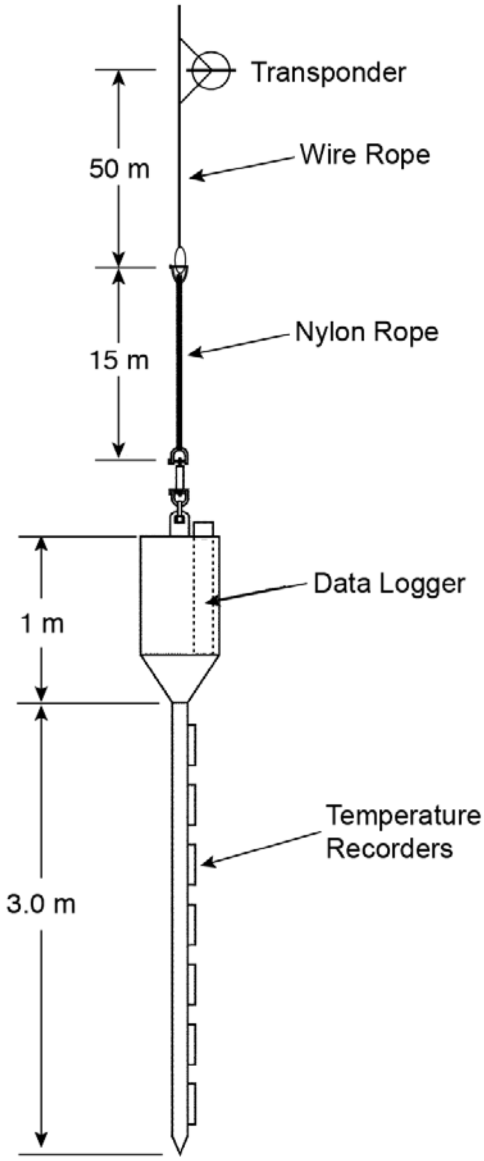

Figure 3.4-3. Configuration of the heat flow measurement system using a deep-sea probe.

3.4.2. Coring system

3.4.2.1 Heat flow piston coring system

[Specification of tools]

During this cruise, sediment core samples were taken with the heat flow piston coring system (HFPC) (Fig. 3.4-4). This coring system is used for combined operation of measuring heat flow and recovering sediments. The HFPC consists of body (800 kg in weight), 4 m stainless steel barrel with liner tube, a balance and a ϕ 74 mm, long type pilot corer. The general outline of the system is shown in Fig. 3.4-5.

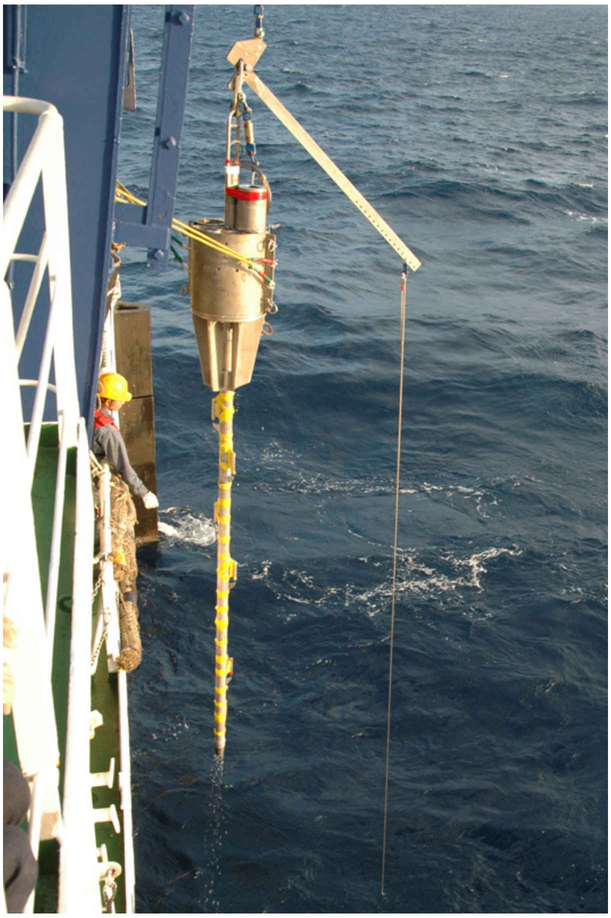

Figure 3.4-4. Heat flow piston coring system (HFPC) with compact temperature data loggers (MTLs).

A stainless steel barrel is attached to a piston core head. The core head has a space for mounting the heat flow data logger to record the temperatures of thermistor sensors mounted along the barrel. On this cruise, seven ANTARES MTLs (cf. 3.4.1) were mounted helically on the outside of barrel, between the base of the weight stand and the core catcher bit. A transponder is also mounted on the winch wire to obtain the depth and position of this equipment.

Nylon rope was placed between the balance and winch wire for additional wire out and/or increased tension after hitting sea bottom. Because the system must be kept in the sediment for 15 minutes to obtain stable temperature, additional wire out is necessary for avoiding pulling the barrel out of the sea floor by either heaving or drifting of the ship during the measurement.

[Preparation for piston coring]

After barrels are attached to the head (weight stand), the main wire is connected, through the barrel, to the piston at the bottom of the barrel. The core catcher and bit are then attached. The balance is connected to the end of the main wire. The entire assemblage is carried under the A-frame using a cart and is lifted over the edge of the deck by the winch, A-frame and capstan winches. The pilot corer and it's wire are then connected to the balance. The system is then lowered through the water to the sea floor.

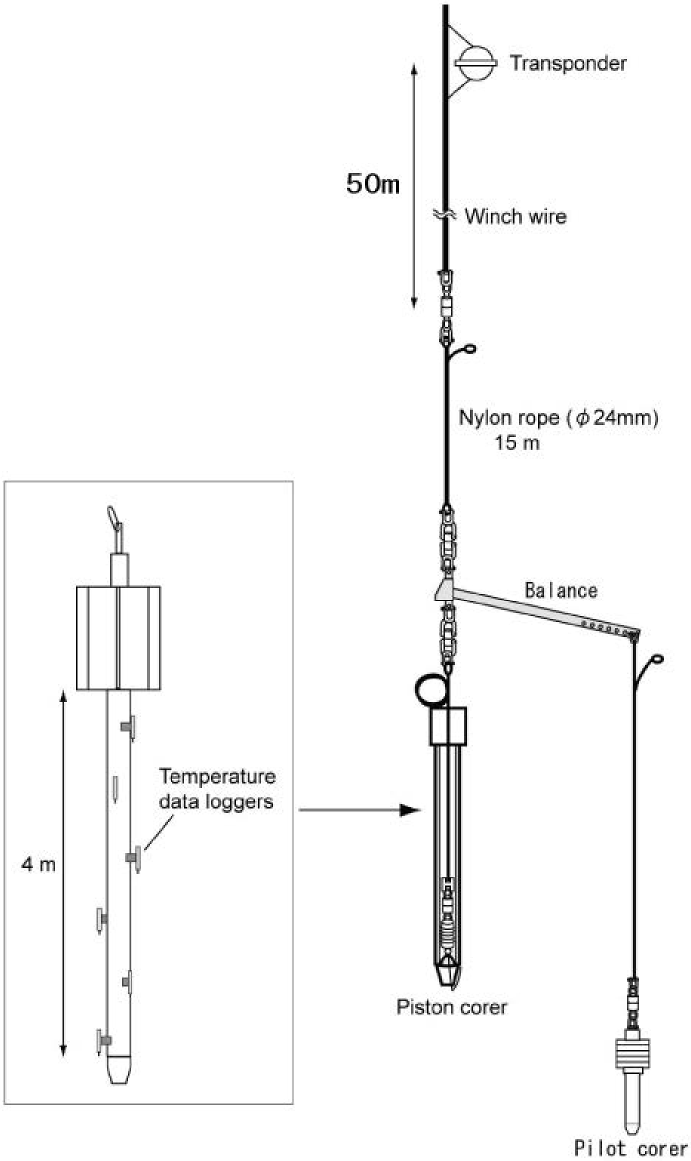

Figure 3.4-5. Configuration of the heat flow piston coring system (HFPC).

[Winch Operations]

The wire out speed is within 60 m/min. The HFPC is stopped at the depth about 100 m above the sea floor, then it is suspended for 5 minutes. After that, the wire is run in 20 m/min.

After the recognition of bottom hit, add about 5 m to wire out, stop and keep the position for 15 minutes. And then, rewinding of the wire is started at a slow speed, until HFPC leaves the sea floor. After we can recognize absolutely that the piston corer is above the sea floor, the wire speed is increased within 60 m/min. The HFPC comes back on the deck, core sample is detached from the body.

3.4.2.2. Gravity coring system

[Specification of tools]

Gravity coring system (GC) consists of body, 7 m stainless steel barrel with liner tube, a balance and a ϕ 74 mm, long type pilot corer (Fig. 3.4-7). Total weight of GC system is 750 kg. A transponder is mounted on the winch wire, 50 m above the GC.

Figure 3.4-6. Gravity coring system (GC).

[Winch Operations]

The wire out speed is within 60 m/min. The GC is stopped at the depth about 100 m above the sea floor, then it is suspended for 5 minutes. After that, the wire is run in 20 m/min. Changes of wire tension value are used to detect GC arrival at or leave from the sea floor. After we can recognize absolutely that the corer is above the sea floor, the wire speed is increased within 60 m/min. The GC comes back on the deck, core sample is detached from the body.

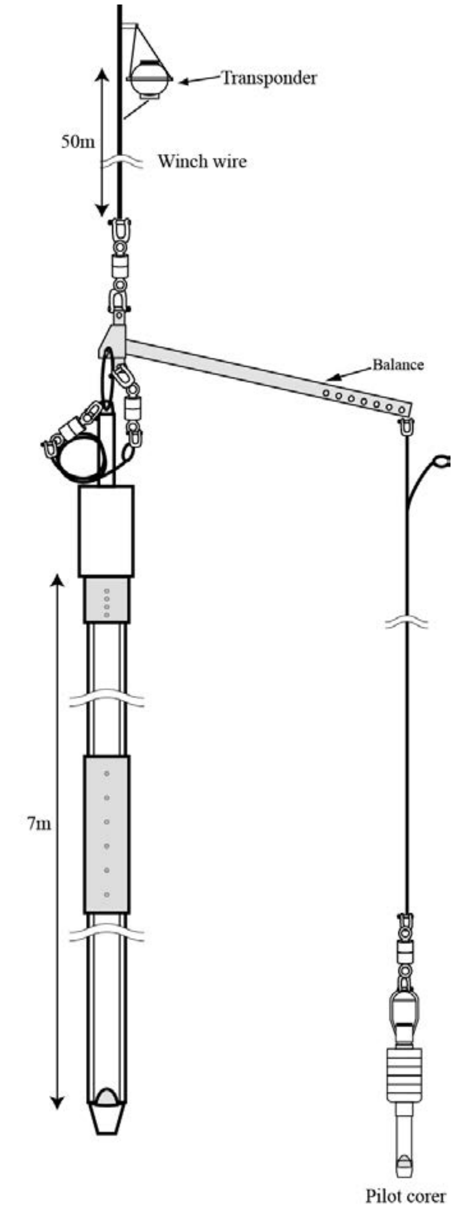

Figure 3.4-7. Configuration of the gravity coring system (GC).

3.4.3. Measurement on core samples

[Thermal property]

Thermal properties (thermal conductivity, heat capacity, and thermal diffusivity) of earth materials are important parameters for calculating heat flow, modeling the thermal structure and transport of heat and fluid under the ground. During the KY13-16 cruise, we used two instruments for thermal property measurement. One is Model QTM-500 (Kyoto Electronics Manufacturing Co., Japan; Fig. 3.4-8), which measures thermal conductivity of sediment with a half space box-type probe (Sass et al., 1984). Measurements with this instrument were made on split core samples. The other is KD2 Pro Thermal Properties Analyzer (Decagon Devices, Inc., USA) with a single needle probe sensor (KS-1 probe) (Von Herzen and Maxwell, 1959) or a dual needle probe sensor (SH-1 probe) (Bristow et al., 1994; Fig. 3.4-9). On this cruise, we inserted dual needle probes into split core samples and measured thermal conductivity, heat capacity, and thermal diffusivity simultaneously.

Figure 3.4-8. Thermal conductivity measurement with QTM-500.

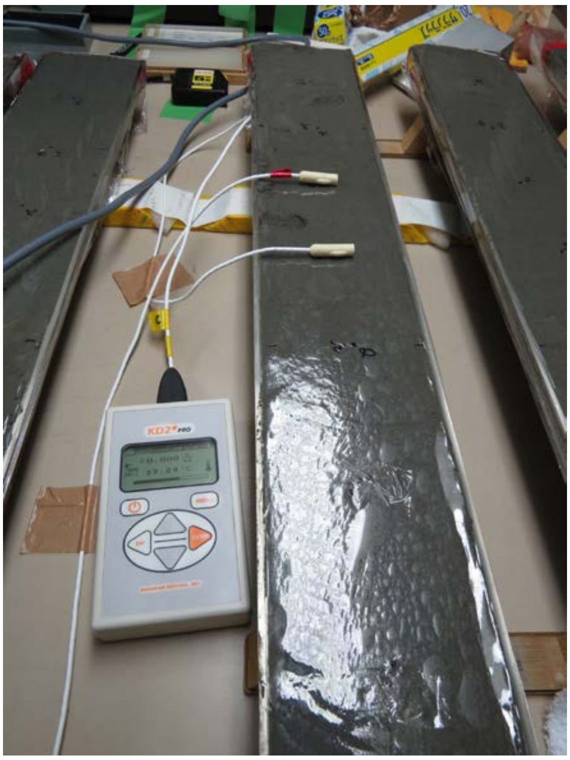

Figure 3.4-9. Thermal conductivity, heat capacity and thermal diffusivity measurement with dual probes of KD2 Pro Thermal Properties Analyzer.

[Sediment color reflectance]

Color reflectance measurements were made onboard at 1 cm resolution on the surface of split cores during the cruise KY13-16 (Fig. 3.4-10). The Minolta CM-2022 spectrophotometer was used to measure the hue and chroma attributes of the sediments as well as the reflected visible light in 31, 10-nm-wide bands ranging from 400 to 700 nm. The sediment colors were expressed in the L*, a* and b* color space indexes. The lightness (variable L*) is ranging from 0% (black) to 100% (white). Variable a* is the green (negative) to red (positive) axis, and variable b* is the blue (negative) to yellow (positive). Color measurement was done within a few hours after split the cores, because color of the surface sediment touched with air is changed rapidly by oxidizing of the organic materials and volatilization of pore water in the sediments.

Before measurement of sample, two calibrations: “the zero calibration” and “white calibration” were carried out. The first one is performed to compensate for the effects of stray light owning to flare characteristics. In addiction, zero calibration may also compensate variations on the ambient such as temperature and humidity. It was performed in the air. The white calibration sets the maximum reflectance to 100%. Each time the camera is switched on and after zero calibration, white calibration was performed. After the regular calibration and white calibration (used in each core measure), the process of measure starts, getting one measure in each 1 cm of the core. After each core section measure, the data was saved and processed by software “Sai-check”, and exported to text file that could be loaded by any spreadsheet software such as MS Excel.

Figure 3.4-10. Sediment color reflectance measurement on the sample KY13-16-HFPC03 with CM-2022 spectrophotometer.

3.5. Preliminary Results

3.5.1. Heat flow measurement

We carried out heat flow measurements at thirteen sites with the deep-sea heat flow probe (Fig. 3.5-1) and at three sites with the HFPC (Table 3.5-1; Figs. 3.2-2 and 3.2-3). At the stations with the deep-sea heat flow probe (HF01 to HF13), multiple penetrations were made for examining local variability of heat flow. The coordinates of the stations listed in Table 3.5-1 are the positions of the acoustic transponder attached above the probe or HFPC determined with the SSBL system of the ship. The water depth in the table is the depth right below the ship determined with the multi-narrow beam echo sounder and may be slightly different from the depth at the station.

Figure 3.5-1. Heat flow measurement operation.

HF01 is located on the northern flank of a bathymetric high, the Kashinosaki Knoll and lies between IODP Sites C0011 and C0012 (cf. 3.3). Heat flow measurements had been successfully made on the lower part of the flank on the KY12-14 cruise and we attempted to add more data on the upper part. We could penetrate the probe at HF01A and B, but the other trials (HF01C to G) were not successful probably because of coarse surface sediment on the upper part of the knoll.

HF02 to HF13 and HFPC03 are on the floor of the Nankai Trough between 133.5°E and

135°E. Although the trough floor is generally flat and covered by soft sediment, heat flow measurement can be made only in very limited spaces because of densely laid submarine telecommunication cables, in the vicinity of which we cannot penetrate probes or corers. The probe or corer fully penetrated into sediments at all the trough floor sites except HF05.

HFPC01 is located on the Nankai accretionary prism and HFPC02 is on the northern margin of the Shikoku Basin just south of the Nankai Trough. At HFPC02, the corer fell down within one minute after hitting the bottom and we could not obtain useful temperature data. It seems that the core barrel could not penetrate deep into sediment due to a volcanic ash layer at a shallow depth (cf. 3.5.2).

Table 3.5-1. Results of heat flow measurements

Date	Station	Latitude (N)	Longitude (E)	Depth (m)	N
Deep-sea heat flow probe					
Oct. 28	HF01A	32°47.52'	136°55.54'	3870	5
	B	32°47.18'	136°55.66'	3850	3
	C	32°46.74'	136°55.80'	3805	fell
	D	32°46.72'	136°55.82'	3805	fell
	E	32°46.23'	136°55.95'	3740	fell
	F	32°45.72'	136°56.03'	3665	fell
	G	32°45.69'	136°56.06'	3665	fell
Oct. 29	HF02A	32°03.00'	134°35.14'	4845	7
	B	32°03.12'	134°35.27'	4845	7
Oct. 30	HF03A	31°46.02'	134°08.00'	4880	7
	B	31°46.02'	134°08.01'	4880	7
	HF04A	31°54.40'	134°19.10'	4885	7
	B	31°54.40'	134°19.10'	4885	7
Oct. 31	HF05A	31°46.49'	133°52.97'	4895	3
	B	31°46.56'	133°52.98'	4895	3
Nov. 1	HF06A	31°33.50'	133°37.47'	4905	7
	B	31°33.51'	133°37.47'	4905	7
	HF07A	31°37.70'	133°47.00'	4905	7
	B	31°37.70'	133°46.99'	4905	7
Nov. 2	HF08A	31°46.51'	134°14.46'	4845	7
	B	31°46.52'	134°14.46'	4845	7

	Date	Station	Latitude (N)	Longitude (E)	Depth (m)	N
	Nov.. 3	HF09A	31°39.99'	133°51.99'	4895	7
		B	31°39.99'	133°51.99'	4895	7
	Nov. 4	HF10A	31°58.80'	134°27.49'	4860	7
		B	31°58.80'	134°27.51'	4855	7
		HF11A	32°05.69'	134°39.92'	4845	7
		B	32°05.69'	134°39.92'	4845	7
	Nov. 5	HF12A	32°08.68'	134°45.48'	4840	7
		B	32°08.68'	134°45.50'	4840	7
		HF13A	32°11.93'	134°50.91'	4830	7
		B	32°11.92'	134°50.90'	4830	7
HFPC						
	Oct. 29	HFPC01	32°21.50'	134°23.00'	2435	5
	Nov. 2	HFPC02	32°32.02'	134°10.01'	4685	fell
	Nov. 3	HFPC03	31°35.71'	133°42.50'	4905	7

N: number of temperature sensors used to obtain temperature profile in sediment.

Heat flow values will be obtained by combining the measured temperature profiles with thermal conductivity of surface sediment. Thermal conductivity at each site needs to be estimated from the values measured on piston core samples and the existing data at nearby stations.

3.5.2. Core samples

Three piston cores and a gravity core were collected from the Nankai Trough area off Shikoku using a 4-m-piston-corer system operated by Marine Works Japan Co. Ltd. (cf. 3.4.2) (Table 3.5-2, Fig. 3.2-2). Seven temperature recorders for heat flow measurement were attached on the core barrel of the piston corer. The piston corer system has a pilot corer (so-called a Marine Work 74 Gravity Corer). We call this system as a heat-flow piston corer (hereafter HFPC).

Each core sample was processed as follows;

1) Cut the whole core into 1-m sections.
2) Split the whole core into Working and Archive halves.
3) Archive half: take photographs, describe sedimentary structures by naked eyes and smear slides.
4) Measure sedimentary color using a Minolta CM-2022 spectrophotometer (cf. 3.4.3).

5) Working half: measure thermal properties using a half-space probe and needle probes (cf. 3.4.3).
6) Seal cores into plastic tube using a vacuum sealer, then pack cores into plastic cases (D-tubes) for storage. Cores were transported to the Kochi Core Center after the cruise.

Table 3.5-2. Core sites during the KY13-16

Core ID onboard	Core Name	Latitude	Longitude	Water depth (m)	Location	Recovery (cm)	No of Section	Major lthology
KY13-16-HFPC01	KY13-16-PC01	32°21.507'N	134°22.990'E	2,432	Nankai Trough continental slope	262	3	Nannofossil silty clay
KY13-16-GC01	KY13-16-GC01	32°08.703'N	133°51.812'E	2,704	Nankai Trough continental slope	357	4+cc	Nannofossil silty clay
KY13-16-GCPL01	KY13-16-GC01-PL	32°08.703'N	133°51.812'E	2,704	Nankai Trough continental slope	16.5	1	Nannofossil silty clay
KY13-16-HFPC02	KY13-16-PC02	31°32.012'N	134°10.036'E	4,682	Nankai Trough	46.5	3	Clay
KY13-16-HFPL02	KY13-16-PC02-PL	31°32.012'N	134°10.036'E	4,682	Nankai Trough	57	1	Clay
KY13-16-HFPC03	KY13-16-PC03	31°35.711'N	133°42.507'E	4,818	Nankai Trough	302	3	Clay to Nannofossil Clay
KY13-16-HFPL03	KY13-16-PC03-PL	31°35.711'N	133°42.507'E	4,818	Nankai Trough	127	2+cc	Nannofossil Clay

3.5.2.1. Thermal properties

Thermal conductivities of sediments were measured with QTM-500 at 8 locations on HFPC01 split core samples, 11 locations on GC01 split core samples, and 8 locations on HFPC03 split core samples (5 on main core samples and 3 on pilot core sample). With dual probes of KD2 Pro Thermal Properties Analyzer, three thermal properties (thermal conductivity, thermal diffusivity and heat capacity) of sediments were measured at 19 locations on HFPC01 split core samples, 29 locations on split core samples of GC01, and 19 locations on split core samples of HFPC03 (14 on main core samples and 5 on pilot core sample).

3.5.2.2. Visual core description and color reflectance

[HFPC01]

HFPC01 was collected from a terrace on the lower continental slope off Muroto Cape in the Nankai Trough (Table 3.5-2, Fig. 3.2-2). The longitude and latitude of the coring site are the average position of the acoustic transponder attached above the HFPC determined with the SSBL system of the ship. The water depth at the coring site is the depth right below the ship determined with the multi-narrow beam echo sounder.

The recovered core sample is 262 cm long. The piston core sediments are predominantly homogenous olive black (10Y3/2), nannofossil silty clay (Figs. 3.5-2 and 3.5-3). Uppermost sediments above ~13 cm are olive brown (2.5Y4/3) nannofossil silty clay, which corresponds to the oxidized layer on the seafloor. Sand sized white pumiceous layer is observed at interval from 44 cm to 47 cm. Pebble sized pumice is found in this pumiceous layer. Color indices L*, a* and b* show that sedimentary color significantly changes at approximately 13 cm and

52.5 cm, respectively (Fig. 3.5-4).

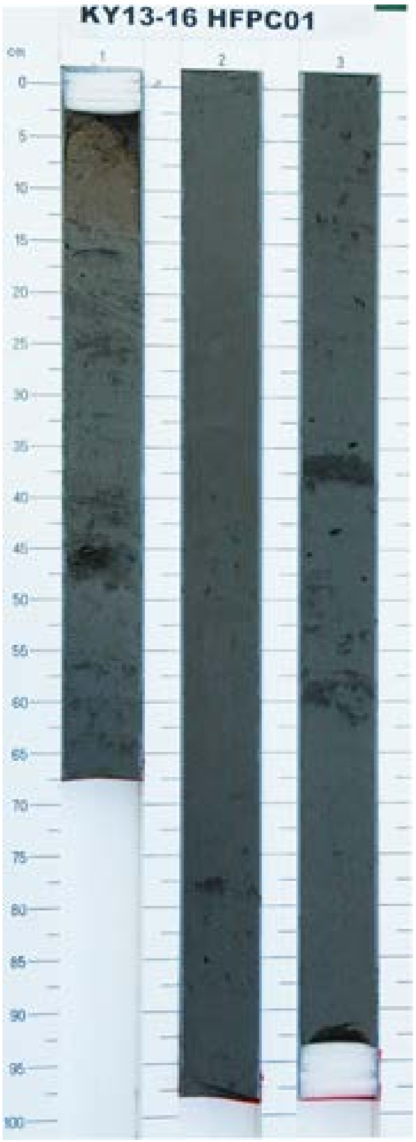

Figure 3.5-2. Photograph of the archive halves of core HFPC01.

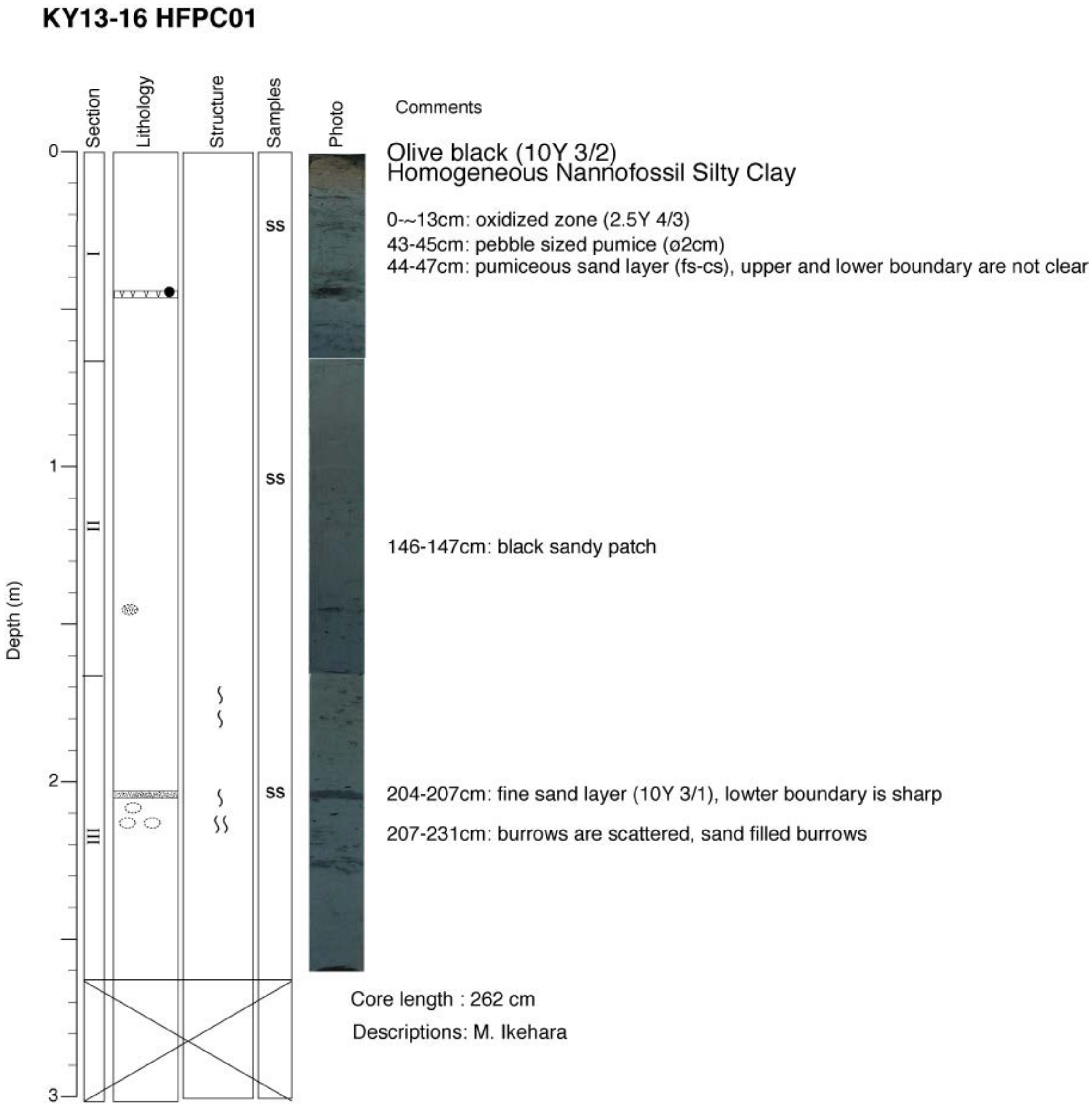

Figure 3.5-3. Summary of visual core description of core HFPC01.

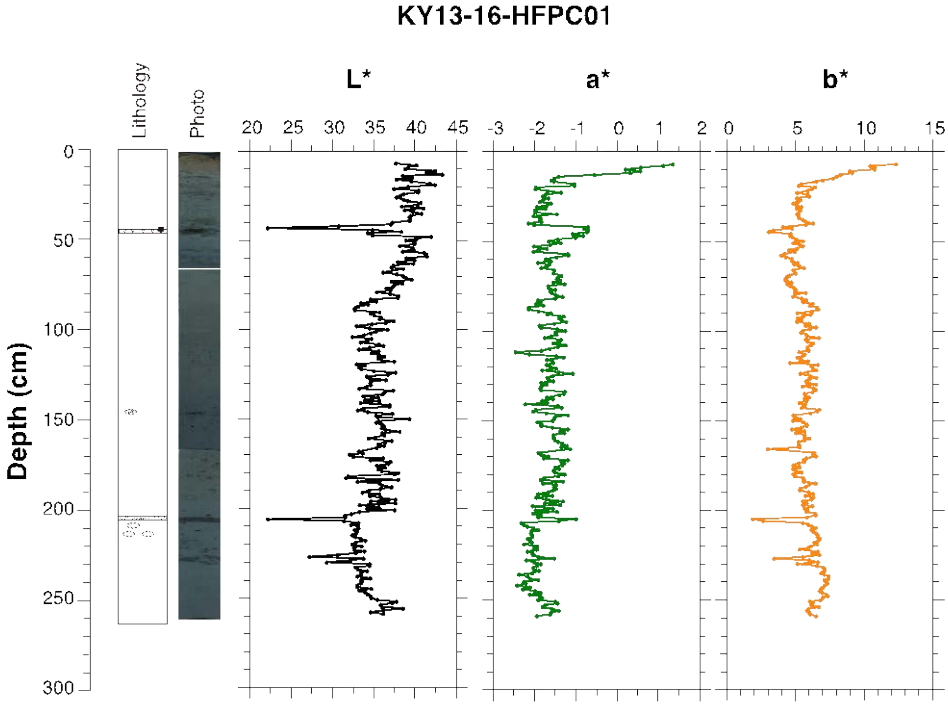

Figure 3.5-4. Color reflectance profiles of core HFPC01.

[GC01 and GCPL01]

GC01 and GCPL01 were collected from a terrace on the lower continental slope in the Nankai Trough (Table 3.5-2, Fig. 3.2-2). The longitude and latitude of the coring site are the average position of the acoustic transponder attached above the GC determined with the SSBL system of the ship. The water depth at the coring site is the depth right below the ship determined with the multi-narrow beam echo sounder.

The recovered core sample of GC01 is 357 cm long. The sediments are predominantly homogenous olive black (10Y3/2), nannofossil silty clay (Figs. 3.5-5 and 3.5-6). Uppermost sediments above ~8 cm are olive brown (2.5Y4/3) nannofossil silty clay, which corresponds to the oxidized layer on the seafloor. Brownish volcanic glass layer is observed at interval from ~76.5 cm to 81.5 cm in this core. A 16.5 cm long pilot core (GCPL01) is composed of homogeneous olive black nannofossil silty clay.

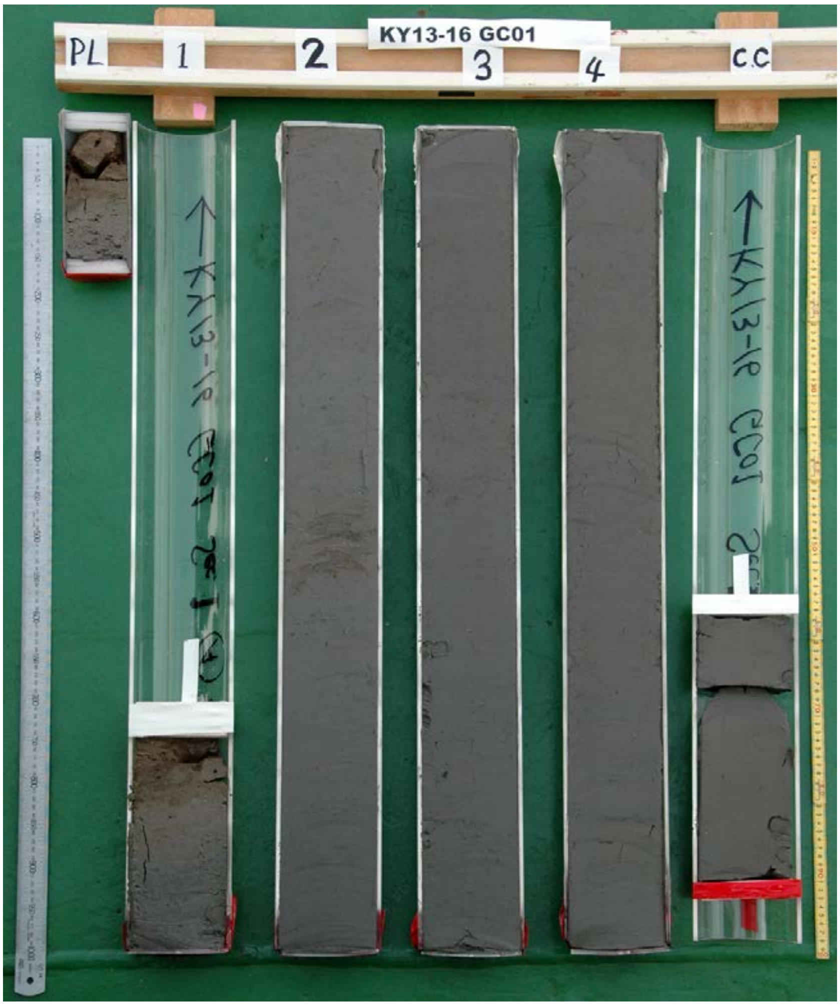

Figure 3.5-5.   Photograph of the archive halves of pilot core GCPL01 and gravity core GC01.

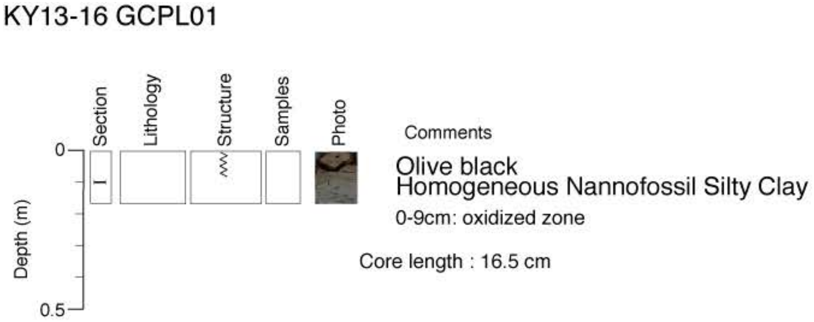

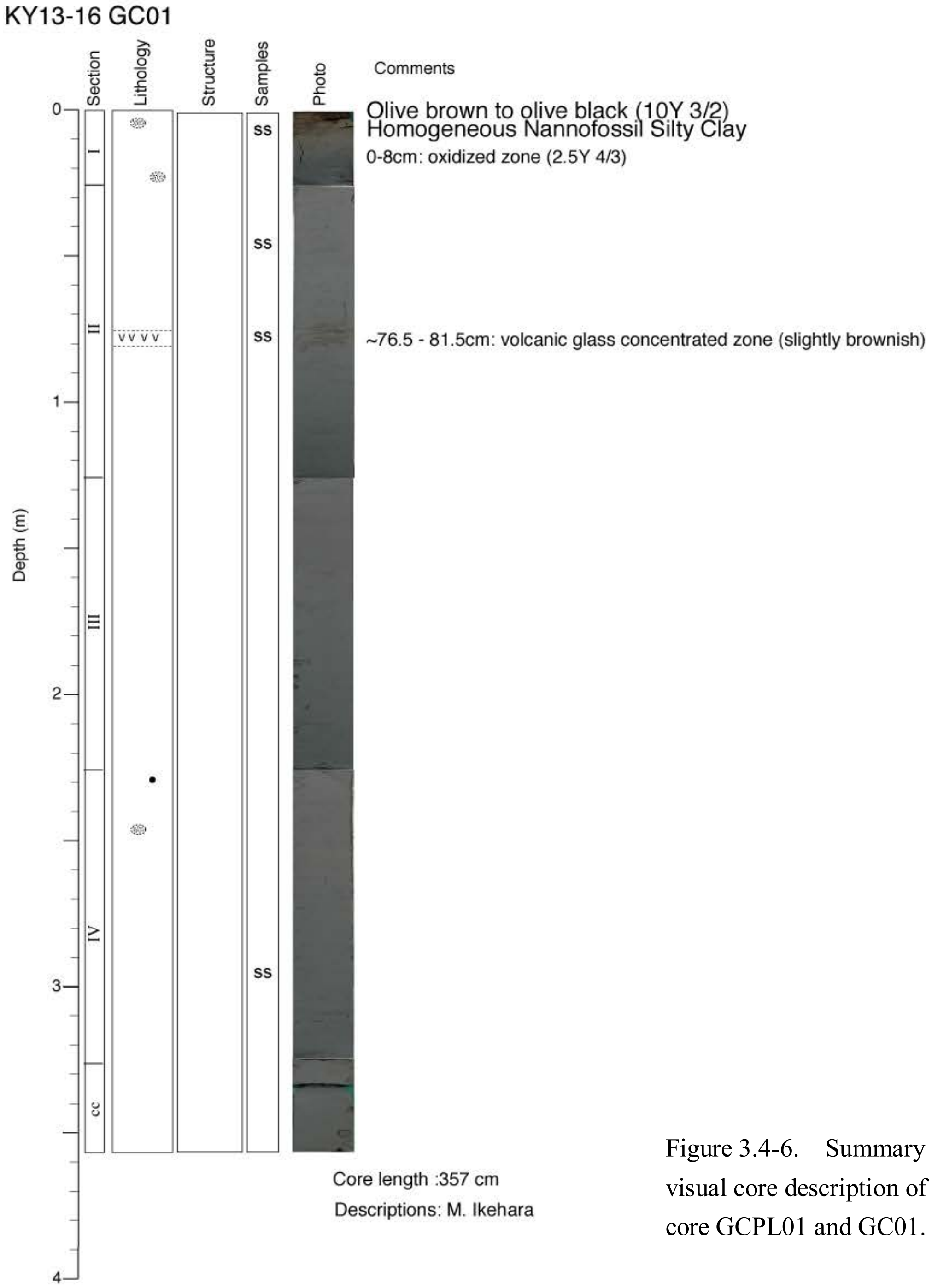

Figure 3.4-6. Summary of visual core description of core GCPL01 and GC01.

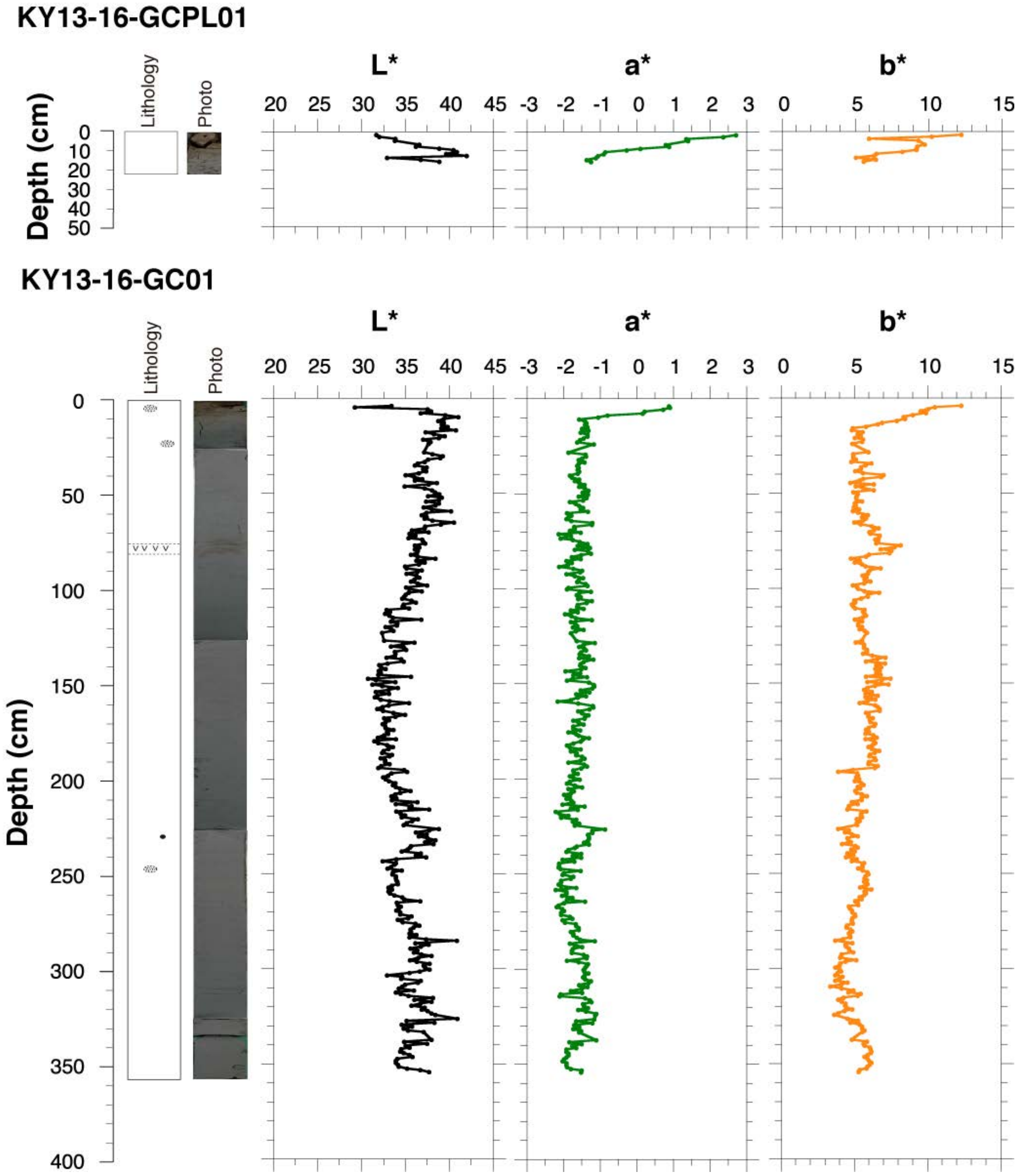

Figure 3.5-7. Color reflectance profiles of core GCPL01 and GC01.

[HFPC02 and HFPL02]

The recovery of pilot core HFPL02 is 46 cm long (Figs. 3.5-8, 3.5-9 and 3.5-10). The sediments are composed of homogeneous dark olive brown (2.5Y 3/3) clay. Volcanic sand patch and ash layer are observed in the lower part of the core (Fig. 3.5-9). Core recovery of HFPC02 is 57 cm long and sedimentary compositions are almost same for HFPL02 (Fig. 3.5-9).

Figure 3.5-8. Photograph of the working halves of pilot core HFPL02 and piston core HFPC02.

KY13-16 HFPL02

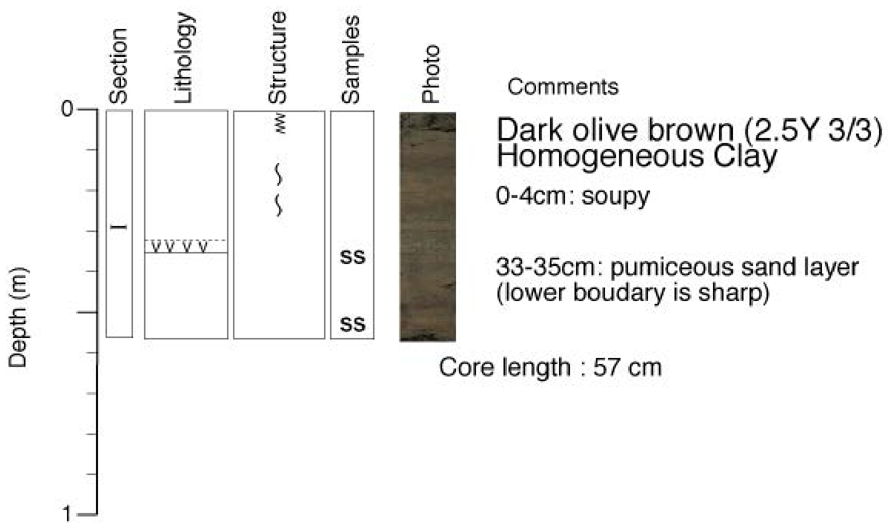

KY13-16 HFPC02

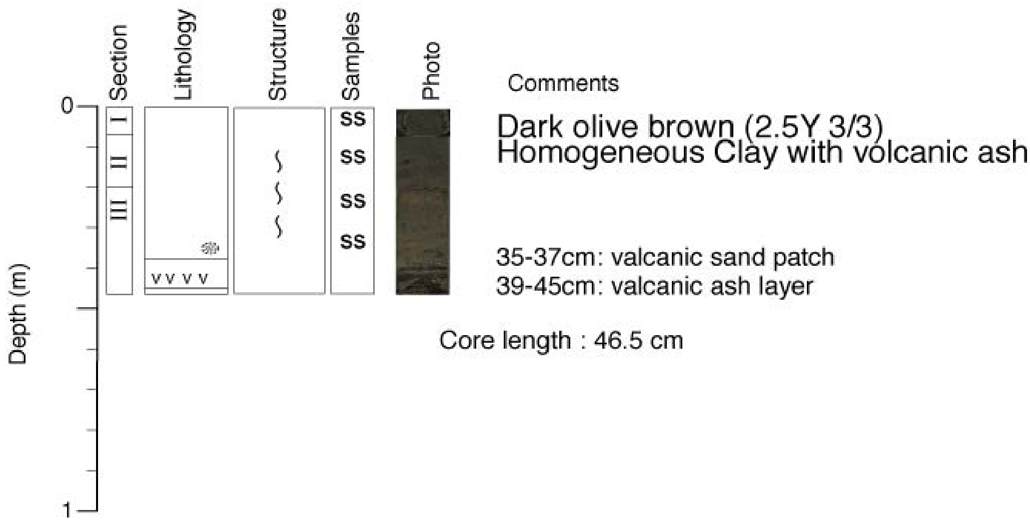

Figure 3.5-9. Summary of visual core description of cores HFPL02 and HFPC02.

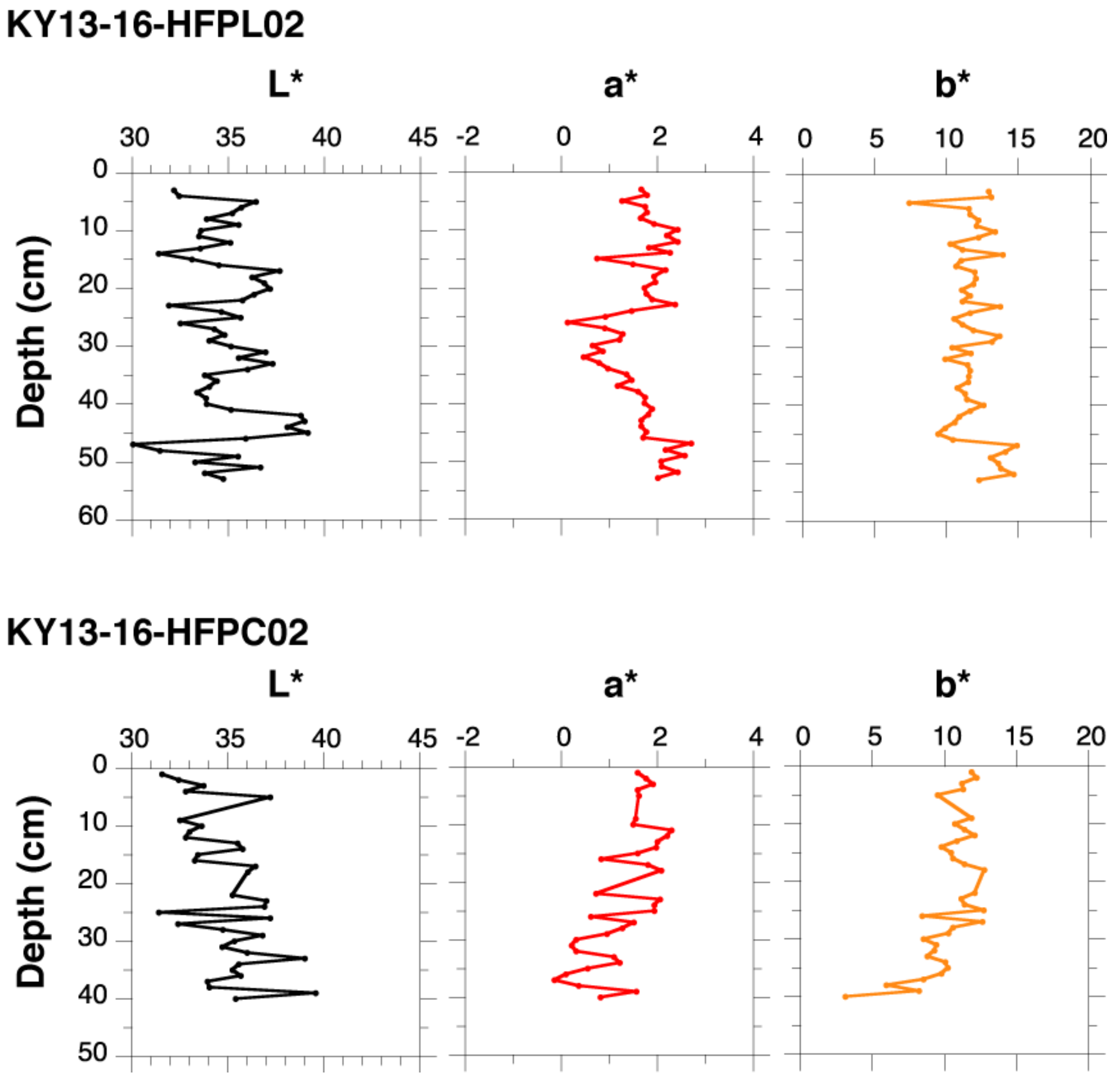

Figure 3.5-10.　Color reflectance profiles of cores HFPL02 and HFPC02.

[HFPC03 and HFPL03]

The recovery of pilot core HFPL03 is 127 cm long (Figs. 3.5-11 and 3.5-12).　The sediments are composed of homogeneous olive black (10Y 3/2) nannofossil clay.　Two sandy patches are observed in the lower part of the core.　Core recovery of HFPC03 is 302 cm long (Figs. 3.5-11 and 3.5-12).　Main lithology is homogeneous clay to nannofossil clay in the core. Upper 4 cm section corresponds to the oxidized layer.　A volcanic ash layer is observed in the lower part (266-276 cm) of the core.　The ash layer shows the fining upward sequence (coarse sand to fine sand).　Based on tentative correlation of sedimentary color (Fig. 3.5-13) and smear slide observation between HFPL03 and HFPC03, surface sediments were not obtained in the pilot core HFPL03, because the body of pilot corer was also penetrated into the sediments due to soft sediments in the western Nankai Trough.

Figure 3.5-11. Photograph of the archive halves of pilot core HFPL03 and piston core HFPC03.

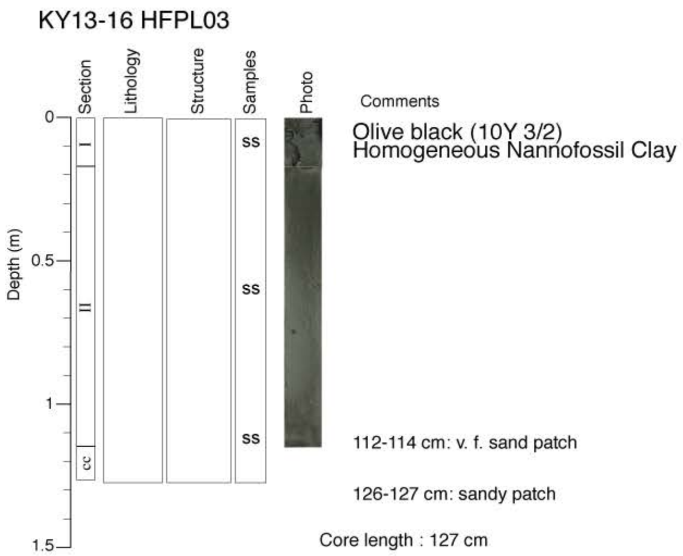

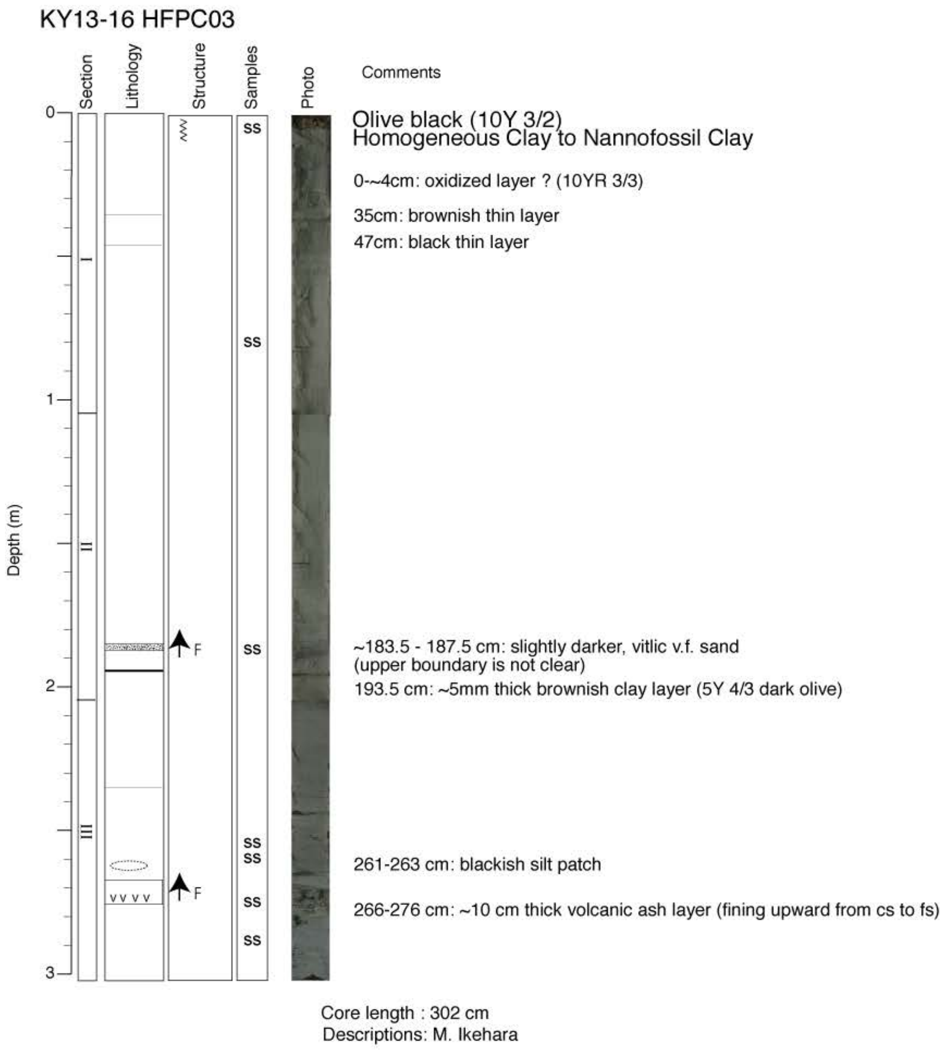

Figure 3.5-12. Summary of visual core description of cores HFPL03 and HFPC03.

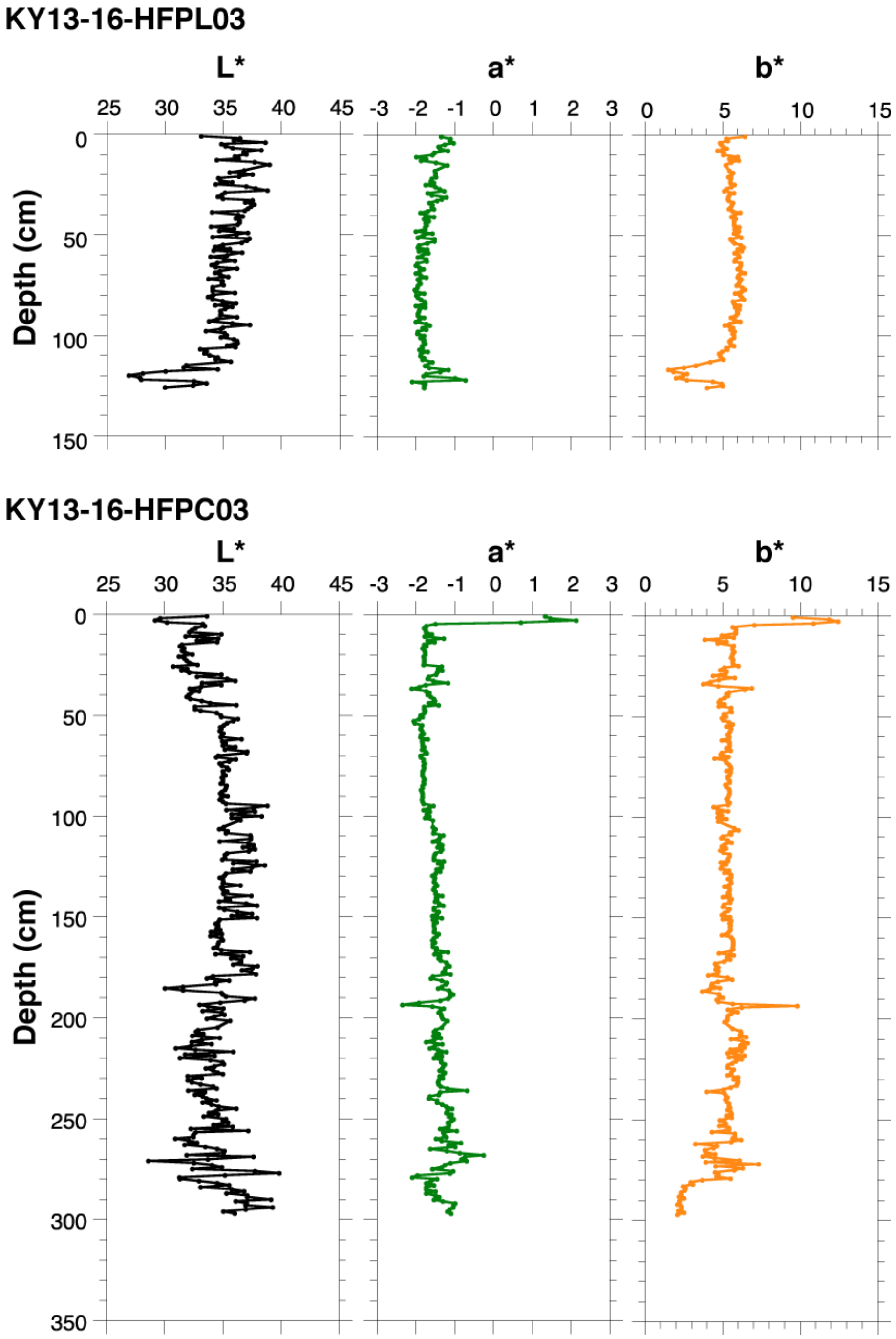

Figure 3.5-13. Color reflectance profiles of cores HFPL03 and HFPC03.

3.5.3. Bathymetry survey

Bathymetry mapping surveys were made at night using a multibeam echo sounding system, SeaBeam 2112 (cf. 7.2). We could fill up most of the blanks in the existing multibeam bathymetry data around the Nankai Trough axis between 133°E and 135.3°E (Fig. 3.5-14).

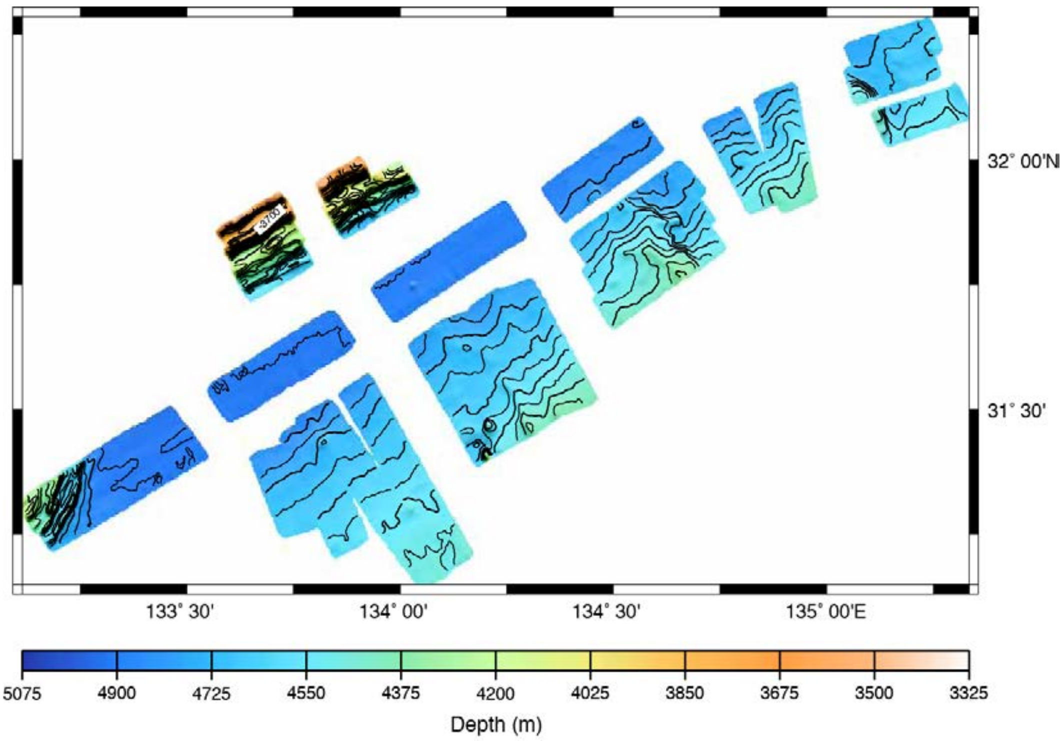

Figure 3.5-14. Topography data obtained through bathymetry surveys during the KY13-16 cruise.

4. Notice on Using

This cruise report is a preliminary documentation as of the end of the cruise.

This report may not be corrected even if changes on contents (i.e. taxonomic classifications) may be found after its publication. This report may also be changed without notice. Data on this cruise report may be raw or unprocessed. If you are going to use or refer to the data written on this report, please ask the Chief Scientist for latest information.

Users of data or results on this cruise report are requested to submit their results to the Data Management Group of JAMSTEC.

5. Acknowledgements

We are grateful to Captain E. Ukekura, the officers and the crew of the R/V KAIYO for skillful operations of the ship and research equipment. We also extend our thanks to M. Toizumi, H. Hayashi, Y. Miyajima, Y. Yamada, and M. Yamaguchi for giving us great assistance in research works throughout the cruise. The staff of the Research Fleet Department, Marine Technology and Engineering Center, especially K. Yatsu, made excellent arrangements for the cruise.

The research conducted on this cruise was partly supported by Ministry of Education, Culture, Sports, Science and Technology through Grant-in Aid for Scientific Research (21107003).

6. References

Bristow, K.L., G.J. Kluitenberg, and R. Horton, Measurement of soil thermal properties with a dual-probe heat-pulse technique, Soil Sci. Soc. Am. J., 58, 1288-1294, 1994.

Fisher, A.T., Marine hydrogeology: recent accomplishments and future opportunities, Hydrogeol. J., 13, 69-97, 2005.

Hamamoto, H., M. Yamano, S. Goto, M. Kinoshita, K. Fujino, and K. Wang, Heat flow distribution and thermal structure of the Nankai subduction zone off the Kii Peninsula, Geochem. Geophys. Geosyst., 12, Q0AD20, doi: 10.1029/2011gc003623, 2011.

Henry, P., T. Kanamatsu, K.T. Moe, M. Strasser and the IODP Expedition 333 ScientificParty, IODP Expedition 333: Return to Nankai Trough subduction inputs sites and coring of mass transport deposits, Scientific Drilling, 14, 4-17, 2012.

Ike, T., G.F. Moore, S. Kuramoto, J.-O. Park, Y. Kaneda, and A. Taira, Variations in sediment thickness and type along the northern Philippine Sea Plate at the Nankai Trough, Island Arc, 17, 342-357, 2008.

Ikehara, M., M. Murayama, O. Tadai, N. Hokanishi, N. Daido, H. Kawahata, and H. Yasuda, Late Quaternary tephrostratigraphy of two IMAGES cores taken from the off Shikoku in the Northwest Pacific, Fossils, 79, 60-76, 2006 (in Japanese with English abstract).

Ikehara, M., D. Akita, and A. Matsuda, Enhanced marine productivity in the Kuroshio region off Shikoku during the last glacial period inferred from the accumulation and carbon isotopes of sedimentary organic matter, J. Quaternary Sci., 24, 848-855, 2009.

Kido, Y. and T. Fujiwara, Regional variation of magnetization of oceanic crust subducting beneath the Nankai Trough, Geochem. Geophys. Geosyst., 5, Q03002, doi:10.1029/2003gc000649, 2004.

Mochizuki, K., K. Nakahigashi, A. Kuwano, T. Yamada, M. Shinohara, S. Sakai, T. Kanazawa, K. Uehira, and H. Shimizu, Seismic characteristics around the fault segment boundary of historical great earthquakes along the Nankai Trough revealed by repeated long-term OBS observations, Geophys. Res. Lett., 37, L09304, doi: 10.1029/2010gl042935, 2010.

Obana, K., S. Kodaira, and Y. Kaneda, Seismicity related to heterogeneous structure along the western Nankai trough off Shikoku Island, Geophys. Res. Lett., 33, L23310, doi:10.1029/2006gl028179, 2006.

Obara, K., Characteristics and interactions between non-volcanic tremor and related slow earthquakes in the Nankai subduction zone, southwest Japan, J. Geodynamics, 52, 229-248, 2011.

Okino, K., Y. Shimakawa, and S. Nagaoka, Evolution of the Shikoku Basin, J. Geomag. Geoelectr., 46, 463-479, 1994.

Sagawa, T., Y. Yokoyama, M. Ikehara, and M. Kuwae, Vertical thermal structure history in the western subtropical North Pacific since the last glacial maximum, Geophys. Res. Lett., 38, L00F02, doi:10.1029/2010GL045827, 2011.

Sass, J.H., C. Stone, and R.J. Munroe, Thermal conductivity determinations on solid rocks - a comparison between a steady-state divided-bar apparatus and a commercial transient line-source device, Jour. Volcanol. Geotherm. Res., 20, 145-153, 1984.

Spinelli, G.A. and K. Wang, Effects of fluid circulation in subducting crust on Nankai margin seismogenic zone temperatures, Geology, 36, 887-890, 2008.

Von Herzen, R. and A.E. Maxwell, The measurement of thermal conductivity of deep-sea sediments by a needle-probe method, J. Geophys. Res., 64, 1557-1563, 1959.

Yamano, M., J.P. Foucher, M. Kinoshita, A. Fisher and R. D. Hyndman, Heat flow and fluid flow regime in the western Nankai accretionary prism, Earth Planet. Sci. Lett., 109, 451-462, 1992

Yamano, M., M. Kinoshita, S. Goto, and O. Matsubayashi, Extremely high heat flow anomaly in the middle part of the Nankai Trough, Phys. Chem. Earth, 28, 487-497, 2003.

Yamano, M., Y. Kawada, S. Goto, and H. Hamamoto, Heat flow distribution on the Nankai Trough floor and its relation to the structure of the Shikoku Basin oceanic crust, AOGS-AGU (WPGM) Joint Assembly 2012, SE52-A015 (abstract), 2012.

7. Appendices

7.1. Cruise Log

Date	Local Time	Note	Position/Weather/Wind/ Sea condition
27-Oct-13		**Sail out, proceeding to research area**	10/27 12:00 (UTC+9h)
	08:50	Boarded by tag boat at YOKOSUKA port.	35-01.2'N, 139-24.9'E
	09:00	Let go all shore line, left YOKOSUKA for research area	Sagami Bay
	10:00-11:00	Briefing about ship's life and safety	bc (Fine but Cloudy)
	13:00-13:15	Practiced life boat, fire and collision station drill	NNE-4 (Moderate breeze)
	16:40	The Kom'pira-san Ceremony, praying for a safe and successful cruise	2 (Sea smooth)
	18:30-19:00	Science meeting	1 (Low swell Short or Average)
			Visibly: 8'
28-Oct-13		**Carried out HF operation**	10/28 12:00 (UTC+9h)
	05:30	Arrived at the research area B	32-46.7'N, 136-55.8'E
	06:41	Released XBT at <32-47.490'N, 136-55.500'E>	Nankai Trough area B
	07:01-17:28	Carried out heat flow measurement <HF01>.	bc (Fine but Cloudy)
	17:30	Proceed to the next research area (Area A).	North-3 (Gentle breeze)
	18:30-18:45	Science meeting	2 (Sea smooth)
			1 (Low swell Short or Average)
			Visibly: 8'
29-Oct-13		**Carried out HFPC & HF operation, MBES survey**	10/29 12:00 (UTC+9h)
	06:00	Arrived at the research area A	32-03.0'N, 134-35.2'E
	06:31	Released XBT at <32-21.480'N, 134-22.680'E>	Nankai Trough area A
	07:06-09:44	Carried out heat flow piston coring <HFPC01>.	bc (Fine but Cloudy)
	12:00-17:01	Carried out heat flow measurement <HF02>.	North-5 (Fresh breeze)
	18:30-18:45	Science meeting	3 (Sea slight)
	19:29	Released XBT at < 31-47.622'N, 134-18.120'E>	2 (Long swell Long)
	19:56	Commenced MBES mapping survey.	Visibly: 8'
30-Oct-13		**Carried out HF operation and MBES survey.**	10/30 12:00 (UTC+9h)
	05:40	Finished MBES mapping survey.	31-49.5'N, 134-12.6'E
	07:00-11:24	Carried out heat flow measurement <HF03>.	Nankai Trough area A
	12:47-17:01	Carried out heat flow measurement <HF04>.	bc (Fine but Cloudy)
	17:25	Commenced MBES mapping survey.	North-3 (Gentle breeze)
	18:30-18:45	Science meeting	2 (Sea smooth)
			2 (Long swell Long)
			Visibly: 8'
31-Oct-13		**Carried out GC & HF operation, MBES survey.**	10/31 12:00 (UTC+9h)
	04:54	Finished MBES mapping survey.	31-46.5'N, 133-53.0'E
	07:08-09:26	Carried out gravity core sampling <GC01>.	Nankai Trough area A
	12:06-16:55	Carried out heat flow measurement <HF05>.	bc (Fine but Cloudy)
	18:30-18:45	Science meeting	ENE-4 (Moderate breeze)
	18:46	Released XBT at < 31-34.602'N, 133-39.720'E>	2 (Sea smooth)
	20:05	Commenced MBES mapping survey.	2 (Long swell Long)
			Visibly: 7'
01-Nov-13		**Carried out HF operation and MBES survey.**	11/01 12:00 (UTC+9h)
	00:46	Finished MBES mapping survey.	31-36.3'N, 133-44.0'E
	06:57-11:18	Carried out heat flow measurement <HF06>.	Nankai Trough area A

Date	Local Time	Note	Position/Weather/Wind/ Sea condition
	12:29-16:53	Carried out heat flow measurement <HF07>.	bc (Fine but Cloudy)
	18:23	Commenced MBES mapping survey.	East-4 (Moderate breeze)
	18:30-18:45	Science meeting	2 (Sea smooth)
			1 (Low swell Short or Average)
			Visibly: 8'
02-Nov-13		**Carried out HFPC & HF operation, MBES survey**	11/02 12:00 (UTC+9h)
	03:12	Finished MBES mapping survey.	31-39.2'N, 134-12.5'E
	07:05-11:15	Carried out heat flow piston coring <HFPC02>.	Nankai Trough area A
	12:51-17:08	Carried out heat flow measurement <HF08>.	o (Overcast (Cloud 10))
	18:06	Commenced MBES mapping survey	ESE-4 (Moderate breeze)
	18:30-18:45	Science meeting	2 (Sea smooth)
	21:44	Finished MBES mapping survey	1 (Low swell Short or Average)
			Visibly: 8'
03-Nov-13		**Carried out HFPC & HF operation, MBES survey**	11/03 12:00 (UTC+9h)
	07:04-11:14	Carried out heat flow piston coring <HFPC03>.	31-39.1'N, 133-50.0'E
	12:35-17:05	Carried out heat flow measurement <HF09>.	Nankai Trough area A
	18:30-18:45	Science meeting	o (Overcast (Cloud 10))
	20:00-24:00	MBES mapping survey.	SSE-2 (Light breeze)
			2 (Sea smooth)
			1 (Low swell Short or Average)
			Visibly: 6'
04-Nov-13		**Carried out HF operation and MBES survey.**	11/04 12:00 (UTC+9h)
	06:58-11:21	Carried out heat flow measurement <HF10>.	32-02.8'N, 134-34.2'E
	12:40-17:00	Carried out heat flow measurement <HF11>.	Nankai Trough area A
	17:29	Commenced MBES mapping survey	o (Overcast (Cloud 10))
	18:30-19:00	Science meeting	NW-4 (Moderate breeze)
			3 (Sea Slight)
			2 (Moderate Short)
			Visibly: 7'
05-Nov-13		**Carried out HF operation and MBES survey.**	11/05 12:00 (UTC+9h)
	01:38	Finished MBES mapping survey	32-12.0'N, 134-51.0'E
	06:58-11:22	Carried out heat flow measurement <HF12>.	Nankai Trough area A
	12:18-16:57	Carried out heat flow measurement <HF13>.	bc (Fine but Cloudy)
	17:15	Finished operation, commenced proceeding to WAKAYAMA port.	NNE-6 (Strong breeze)
			4 (Sea Moderate)
			2 (Moderate Short)
			Visibly: 8'
06-Nov-13		**Disembarked at WAKAYAMA**	
	09:00	Disembarked at WAKAYAMA port	

7.2. Bathymetry Survey Lines

Line Name	Start				End			
	Date	Time (UTC)	Latitude	Longitude	Date	Time (UTC)	Latitude	Longitude
Line 1_a	10/29	19:51	31 - 43.029N	133 - 58.028N	10/29	20:40	31 - 47.430N	134 - 06.008N
Line 1_b	10/30	08:25	31 - 53.009N	134 - 16.055N	10/30	09:29	31 - 47.443N	134 - 05.957N
Line 2	10/29	17:27	31 - 24.981N	134 - 13.015N	10/29	19:04	31 - 38.998N	134 - 04.005N
Line 3	10/29	15:24	31 - 41.051N	134 - 08.017N	10/29	16:58	31 - 27.012N	134 - 17.005N
Line 4	10/29	13:14	31 - 29.038N	134 - 20.973N	10/29	14:53	31 - 43.017N	134 - 11.974N
Line 5	10/29	10:57	31 - 44.667N	134 - 16.183N	10/29	12:35	31 - 30.956N	134 - 25.062N
Line 6	10/30	10:57	31 - 40.029N	133 - 52.034N	10/30	12:47	31 - 30.990N	133 - 34.974N
Line 7	10/30	14:11	31 - 45.516N	133 - 38.048N	10/30	14:58	31 - 49.524N	133 - 46.060N
Line 8	10/30	15:17	31 - 52.071N	133 - 45.033N	10/30	16:09	31 - 48.017N	133 - 37.012N
Line 9	10/30	16:27	31 - 50.459N	133 - 35.988N	10/30	17:12	31 - 54.482N	133 - 43.972N
Line 10	10/30	17:47	31 - 53.012N	133 - 50.978N	10/30	18:43	31 - 57.993N	134 - 00.978N
Line 11	10/30	19:20	31 - 58.574N	133 - 55.236N	10/30	19:54	31 - 55.958N	133 - 49.910N
Line 12	10/31	11:05	31 - 26.510N	133 - 30.999N	10/31	13:21	31 - 15.533N	133 - 10.068N
Line 13	10/31	13:41	31 - 17.470N	133 - 07.959N	10/31	15:46	31 - 28.478N	133 - 28.975N
Line 14	11/1	15:49	31 - 11.938N	134 - 08.041N	11/1	18:12	31 - 33.024N	133 - 53.997N
Line 15	11/1	12:54	31 - 29.972N	133 - 48.042N	11/1	15:26	31 - 10.007N	134 - 04.993N
Line 16	11/1	11:33	31 - 18.141N	133 - 50.927N	11/1	12:37	31 - 28.020N	133 - 45.990N
Line 17	11/1	09:23	31 - 25.062N	133 - 41.987N	11/1	10:23	31 - 15.984N	133 - 46.012N
Line 18	11/2	09:06	31 - 55.028N	134 - 22.036N	11/2	10:14	32 - 03.051N	134 - 35.110N
Line 19	11/2	10:59	31 - 58.053N	134 - 41.038N	11/2	12:44	31 - 48.991N	134 - 25.998N
Line 20	11/3	13:00	31 - 54.510N	134 - 42.510N	11/3	15:00	31 - 45.521N	134 - 27.531N
Line 21	11/3	11:03	31 - 42.018N	134 - 29.025N	11/3	12:33	31 - 51.007N	134 - 44.019N
Line 22	11/4	08:29	32 - 05.011N	134 - 45.504N	11/4	09:33	31 - 55.002N	134 - 51.454N
Line 23	11/4	09:57	31 - 55.040N	134 - 56.032N	11/4	11:25	32 - 08.027N	134 - 53.007N
Line 24	11/4	12:23	32 - 12.009N	135 - 04.039N	11/4	13:20	32 - 14.972N	135 - 14.976N
Line 25	11/4	13:44	32 - 12.060N	135 - 14.961N	11/4	15:02	32 - 08.997N	135 - 04.004N
Line 26	11/4	15:40	32 - 04.003N	135 - 07.932N	11/4	16:38	32 - 07.000N	135 - 19.007N

7.3. R/V KAIYO Crew

Captain	EIKO UKEKURA
Chief Officer	TAKAAKI SHISHIKURA
2nd Officer	MASATO CHIBA
3rd Officer	TOMOHIRO YUKAWA
Chief Engineer	TADASHI ABE
1st Engineer	TAKASHI OTA
2nd Engineer	SABURO SAKAEMURA
3rd Engineer	SHOHEI MIYAZAKI
Chief Radio Operator	TAKEHITO HATTORI
2nd Radio Operator	SHUNSUKE FUKAGAWA
3rd Radio Operator	TAKAYUKI MABARA
Boat Swain	KAZUO ABE
Able Seaman	SHUJI TAKUNO
Able Seaman	YUKI YOSHINO
Able Seaman	YOSHIAKI MATSUO
Sailor	HIROTAKA SHIGETA
Sailor	RYOMA TAMURA
Sailor	YUSAKU KANADA
No.1 Oiler	HIROYUKI OISHI
Oiler	KEITA UNAWATARI
Assistant Oiler	MAKOTO KOZAKI
Assistant Oiler	AOI TAKAMIYA
Assistant Oiler	NAOTO MITSUO
Chief Steward	TOMIHISA MORITA
Steward	KAZUHIRO HIRAYAMA
Steward	HIROAKI MORIMOTO
Steward	HARUKA KINOSHITA
Steward	MANAMI TAKAHASHI